EUROPEAN ORGANISATION FOR NUCLEAR RESEARCH (CERN)

Submitted to: Phys. Rev. D

CERN-EP-2018-179
August 8, 2018

Combination of searches for heavy resonances decaying into bosonic and leptonic final states using 36 fb^{-1} of proton–proton collision data at $\sqrt{s}$ = 13 TeV with the ATLAS detector

The ATLAS Collaboration

Searches for new heavy resonances decaying into different pairings of W, Z, or Higgs bosons, as well as directly into leptons, are presented using a data sample corresponding to 36.1 fb^{-1} of pp collisions at $\sqrt{s}$ = 13 TeV collected during 2015 and 2016 with the ATLAS detector at the CERN Large Hadron Collider. Analyses selecting bosonic decay modes in the $qqqq$, $\nu\nu qq$, $\ell\nu qq$, $\ell\ell qq$, $\ell\nu\ell\nu$, $\ell\ell\nu\nu$, $\ell\nu\ell\ell$, $\ell\ell\ell\ell$, $qqbb$, $\nu\nu bb$, $\ell\nu bb$, and $\ell\ell bb$ final states are combined, searching for a narrow-width resonance. Likewise, analyses selecting the leptonic $\ell\nu$ and $\ell\ell$ final states are also combined. These two sets of analyses are then further combined. No significant deviation from the Standard Model predictions is observed. Three benchmark models are tested: a model predicting the existence of a new heavy scalar singlet, a simplified model predicting a heavy vector-boson triplet, and a bulk Randall–Sundrum model with a heavy spin-2 Kaluza–Klein excitation of the graviton. Cross-section limits are set at the 95% confidence level using an asymptotic approximation and are compared with predictions for the benchmark models. These limits are also expressed in terms of constraints on couplings of the heavy vector-boson triplet to quarks, leptons, and the Higgs boson. The data exclude a heavy vector-boson triplet with mass below 5.5 TeV in a weakly coupled scenario and 4.5 TeV in a strongly coupled scenario, as well as a Kaluza–Klein graviton with mass below 2.3 TeV.

1 Introduction

The search for new heavy particles is an important part of the physics program at the Large Hadron Collider (LHC) and has been the focus of an intense effort to uncover physics beyond the Standard Model (SM) in a broad range of final states. Many of these searches are motivated by models aiming to resolve the hierarchy problem such as the Randall–Sundrum (RS) model with a warped extra dimension [1], by models with extended Higgs sectors as in the two-Higgs-doublet model (2HDM) [2], or by models with composite Higgs bosons [3] or extended gauge sectors as in Grand Unified Theories [4–6].

Although no significant excess has been observed to date, strong constraints have been placed on the production of such new heavy particles. A combination of searches for the production of heavy resonances decaying into the VV (with $V = W$ or Z) final state in proton–proton (pp) collisions at a center-of-mass energy $\sqrt{s} = 13$ TeV corresponding to an integrated luminosity of 3.2 fb^{-1} has been published by the ATLAS Collaboration [7]. Similarly, a combination of searches in the VV and VH (with H representing the SM Higgs boson) final states obtained with 19.7 fb^{-1} at $\sqrt{s} = 8$ TeV and 2.7 fb^{-1} at $\sqrt{s} = 13$ TeV has been published by the CMS Collaboration [8]. In this article, the combination is broadened to include the results of not only the VV and VH searches but lepton–antilepton searches as well. It uses the most recent ATLAS results obtained at $\sqrt{s} = 13$ TeV with an integrated luminosity of approximately 36 fb^{-1}. A combination with a broader set of final states allows one to explore the complementarity of these searches and set stronger constraints over a wider range of models of physics beyond the SM. Several diagrams illustrating the production and decay of new heavy resonances are shown in Figure 1.

The specific searches combined in this article are those performed in the VV channels: $WZ \to qqqq$ [9], $\ell\nu qq$ [10], $\ell\nu\ell\ell$ [11], $WW \to qqqq$ [9], $\ell\nu qq$ [10], $\ell\nu\ell\nu$ [12], and $ZZ \to qqqq$ [9], $\nu\nu qq$ [13], $\ell\ell qq$ [13], $\ell\ell\nu\nu$ [14], $\ell\ell\ell\ell$ [14]; the VH channels: $WH \to qqbb$ [15], $\ell\nu bb$ [16], and $ZH \to qqbb$ [15], $\nu\nu bb$ [16], $\ell\ell bb$ [16]; and the lepton–antilepton channels: $\ell\nu$ [17] and $\ell\ell$ [18]. The charged leptons ℓ are either electrons or muons. For the VV and VH decay channels involving leptonic decays of vector bosons, τ-leptons are included as part of the signal since τ-lepton decays into electrons or muons provide a small amount of additional acceptance. The impact of τ-leptons is very small and neglected in other channels. In this article, the VV and VH decay channels are collectively named "bosonic", whereas the lepton–antilepton decay channels are collectively named "leptonic." The analyses generally search for narrow resonances in the final-state mass distribution with the signal shape extracted from Monte Carlo (MC) simulation of specific models. The background shape and normalization are extracted from a combination of MC simulation and data, often relying on dedicated control regions to extract the various background contributions. The mass distributions and associated systematic uncertainties from the various channels are combined taking correlations into account, as described below.

2 Signal models

The results presented in this article are interpreted in the context of three models: the heavy vector triplet (HVT) model [19, 20], the RS model, and an empirical model featuring a new heavy scalar.

The HVT model provides a broad phenomenological framework that encompasses a range of different scenarios involving new heavy gauge bosons and their couplings to SM fermions and bosons. In this model, a triplet $\mathcal{W}$ of colorless vector bosons is introduced with zero hypercharge. This leads to a set of

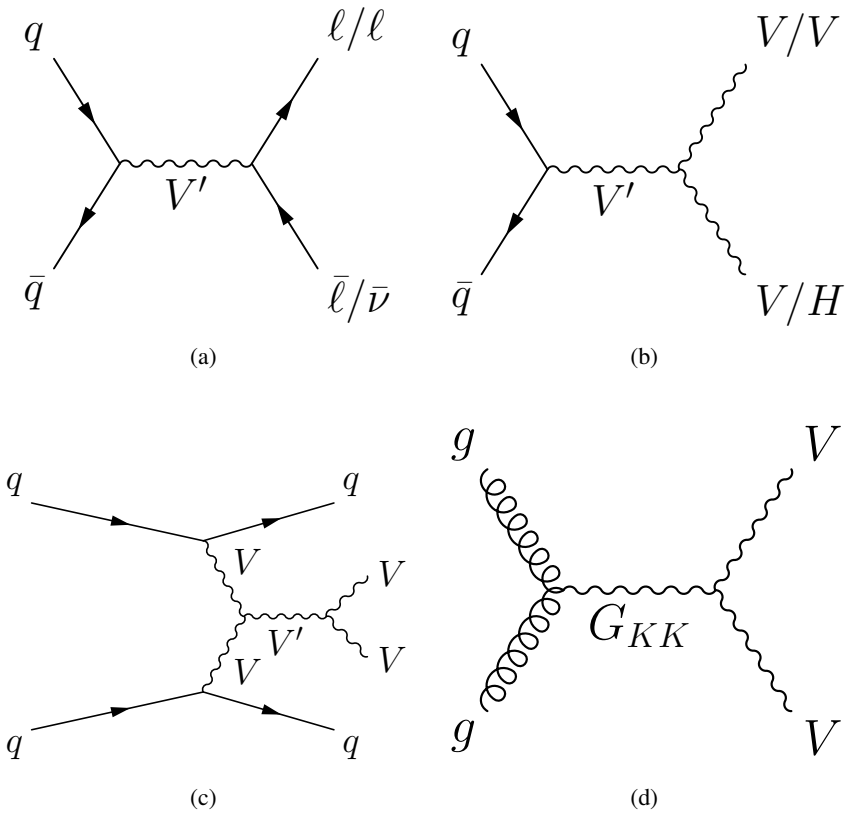

Figure 1: Feynman diagrams for heavy resonance production and decay: (a) Drell–Yan production and decay into $\ell\nu/\ell\ell$, (b) Drell–Yan production and decay into VV/VH, (c) vector-boson fusion production and decay into VV, and (d) gluon–gluon fusion production and decay into VV (with $V = W$ or Z).

nearly degenerate charged, $W'^{\pm}$, and neutral, Z', states collectively denoted by V'.[1] For the interpretation performed in this article, the W' and Z' masses are taken to be the same. The model allows one to explore different coupling strengths of those states to quarks, leptons, vector bosons, and Higgs bosons with the following interaction Lagrangian:

$$\mathcal{L}_{\mathcal{W}}^{\text{int}} = -g_q \mathcal{W}_\mu^a \bar{q}_k \gamma^\mu \frac{\sigma_a}{2} q_k - g_\ell \mathcal{W}_\mu^a \bar{\ell}_k \gamma^\mu \frac{\sigma_a}{2} \ell_k - g_H \left(\mathcal{W}_\mu^a H^\dagger \frac{\sigma_a}{2} i D^\mu H + \text{h.c.} \right), \tag{1}$$

where q_k and ℓ_k represent the left-handed quark and lepton doublets for fermion generation k ($k = 1, 2, 3$); H represents the Higgs doublet; σ_a ($a = 1, 2, 3$) are the Pauli matrices; and g_q, g_ℓ, and g_H correspond to the coupling strengths between the triplet field $\mathcal{W}$ and the quark, lepton, and Higgs fields, respectively.[2] Interactions with fermions of different generations are assumed to be universal and right-handed fermions do not participate. The triplet field interacts with the Higgs field and thus with the longitudinally polarized W and Z bosons by virtue of the equivalence theorem [21–23]. In this framework, the branching fractions

[1] The charged state is denoted W' in the remainder of this article.

[2] The coupling constants g_H, g_f, g_q, and g_ℓ are used in this article. They are related to those in Ref. [20] as follows: the Higgs coupling $g_H = g_V c_H$ and the universal fermion coupling $g_f = g^2 c_F / g_V$, where g is the SM $\text{SU}(2)_\text{L}$ gauge coupling, while the c parameters and the coupling g_V are defined in Ref. [20]. Couplings specific to quarks and leptons are given by $g_q = g^2 c_q / g_V$ and $g_\ell = g^2 c_\ell / g_V$.

for the decays $W' \to WZ$, $W' \to WH$, $Z' \to WW$, and $Z' \to ZH$, are equal for V' masses above 1.5 TeV and other neutral diboson final states are either suppressed or forbidden.

Three explicit HVT scenarios are used as benchmarks for interpretation of the results. The first two benchmarks are both Drell-Yan (DY) production mechanisms (Figures 1(a) and 1(b)), while the third benchmark proceeds via the vector-boson fusion (VBF) mechanism (Figure 1(c)). Within the DY processes, two scenarios differently emphasize the relative strengths of g_H and g_f. The first DY scenario, referred to as model A, reproduces the phenomenology of weakly coupled models based on an extended gauge symmetry [24]. In this case, the couplings are $g_H = -0.56$ and $g_f = -0.55$, with the universal fermion coupling $g_f = g_q = g_\ell$. The second DY scenario, referred to as model B, implements a strongly coupled scenario as in composite Higgs models [3] with $g_H = -2.9$ and $g_f = 0.14$.[3] In model B, the V' resonances are broader than in the weakly coupled scenario, model A, but remain narrow relative to the experimental resolution. The relative width, Γ/m, is below 5% over much of the parameter space explored in this article. Model B is not considered for masses below 1500 GeV because model A is used to extract the acceptance of the combined channels, and the branching fractions to VV and VH differ between models A and B in that mass range. The acceptance for individual channels is the same for models A and B. There is also a second constraint for model B, for masses below 800 GeV, where it is not compatible with SM precision measurements due to increased mixing between the SM gauge bosons and the heavy vector resonance.

For the DY process with decay of the V' into lepton–antilepton final states, branching fractions are largest in model A with values of approximately 4% and only about 0.2% in model B, for each generation taken separately. In contrast, the branching fractions for decays into individual diboson channels are about 2% in model A, whereas they are close to 50% in model B.

The third scenario, referred to as model C, is designed to focus solely on the rare process of vector-boson fusion. In this case, the V' resonance couplings are set to $g_H = 1$ and $g_f = 0$. Model C is therefore in a separate phase space domain to models A and B and assumes no DY production. The interpretation can be extended beyond these three benchmark models by considering the two-dimensional parameter space consisting of g_H and g_f (assuming fermion universality) or g_q and g_ℓ for a given value of g_H. The different production mechanisms and decay modes included here provide sensitivity to different regions of this parameter space, with production via the DY process providing sensitivity to g_q and production via VBF providing sensitivity to g_H. Likewise, decays into lepton–antilepton states provide sensitivity to g_ℓ whereas decays into diboson states provide sensitivity to g_H.

The RS model postulates the existence of a warped extra dimension in which only gravity propagates as in the original "RS1" scenario [1] or in which both gravity and all SM fields propagate as in the "bulk RS" scenario [25]. Propagation in the extra dimension leads to a tower of Kaluza–Klein (KK) excitations of gravitons (denoted G_{KK}) and SM fields. In the bulk RS model considered here, KK gravitons are produced via both quark–antiquark annihilation and gluon–gluon fusion (ggF), with the latter dominating due to suppressed couplings to light fermions. The strength of the coupling depends on $k/\overline{M}_{\mathrm{Pl}}$, where k corresponds to the curvature of the warped extra dimension and $\overline{M}_{\mathrm{Pl}} = 2.4 \times 10^{18}$ GeV is the effective four-dimensional Planck scale. Both the production cross section and decay width of the KK graviton scale as the square of $k/\overline{M}_{\mathrm{Pl}}$. For the value $k/\overline{M}_{\mathrm{Pl}} = 1$ used in the interpretation, the G_{KK} resonance width relative to its mass is approximately 6%. The G_{KK} branching fraction is largest for decays into the $t\bar{t}$ final state, with values ranging from 42% for $m(G_{\mathrm{KK}}) = 0.5$ TeV to 65% for $m(G_{\mathrm{KK}})$ values above

[3] In terms of the coupling constants in the notation of Ref. [20], the choices for models A and B correspond to $g_V = 1$ and $g_V = 3$, respectively.

Table 1: Cross sections for production of heavy resonances of different masses in HVT models A and B via the Drell–Yan process, in HVT model C via vector-boson fusion, and in the bulk RS model via gluon–gluon fusion and the Drell–Yan process.

	HVT model A		HVT model B		HVT model C		Bulk RS
m [TeV]	$\sigma(W')$ [fb]	$\sigma(Z')$ [fb]	$\sigma(W')$ [fb]	$\sigma(Z')$ [fb]	$\sigma(W')$ [fb]	$\sigma(Z')$ [fb]	$\sigma(G_{\mathrm{KK}})$ [fb]
1.0	2.20×10^4	1.12×10^4	987	510	1.30	0.888	583
2.6	219	100	14.0	6.44	4.78×10^{-3}	3.14×10^{-3}	1.41
4.0	9.49	4.37	0.626	0.288	1.27×10^{-4}	7.92×10^{-5}	3.25×10^{-2}

Table 2: Signal models, resonances, and decay modes considered in the combination.

Model \ Decay mode	WW	WZ	ZZ	WH	ZH	$\ell\nu$	$\ell\ell$
HVT	Z'	W'		W'	Z'	W'	Z'
Bulk RS	G_{KK}		G_{KK}				
Scalar	Scalar		Scalar				

1 TeV. Corresponding values for the WW (ZZ) final state range from 34% to 20% (18% to 10%). Table 1 presents production cross sections for several heavy resonance masses in the HVT models A, B, and C, and the bulk RS model.

The last model considered is an empirical model with a narrow heavy scalar resonance produced via the ggF and VBF mechanisms and decaying directly into VV. The width of this new scalar is assumed to be negligible compared with the detector resolution, and the relative branching fractions for decay into the WW and ZZ final states approximately follow a $2:1$ ratio. This benchmark is used to explore sensitivity to extended Higgs sectors. Table 2 summarizes the channels considered in the interpretation for each signal model.

3 ATLAS detector

The ATLAS experiment [26, 27] at the LHC is a multipurpose particle detector with a forward–backward symmetric cylindrical geometry and a near 4π coverage in solid angle.[4] It consists of an inner detector for tracking surrounded by a thin superconducting solenoid providing a 2 T axial magnetic field, electromagnetic and hadronic calorimeters, and a muon spectrometer. The inner detector covers the pseudorapidity range $|\eta| < 2.5$. It consists of silicon pixel, silicon microstrip, and transition-radiation tracking detectors. A new innermost pixel layer [27] inserted at a radius of 3.3 cm has been used since 2015. Lead/liquid-argon (LAr) sampling calorimeters provide electromagnetic (EM) energy measurements with high granularity.

[4] ATLAS uses a right-handed coordinate system with its origin at the nominal interaction point (IP) in the center of the detector and the z-axis along the beam pipe. The x-axis points from the IP to the center of the LHC ring, and the y-axis points upwards. Cylindrical coordinates (r, ϕ) are used in the transverse plane, ϕ being the azimuthal angle around the z-axis. The pseudorapidity is defined in terms of the polar angle θ as $\eta = -\ln\tan(\theta/2)$. Angular distance is measured in units of $\Delta R \equiv \sqrt{(\Delta\eta)^2 + (\Delta\phi)^2}$.

A hadronic (steel/scintillator-tile) calorimeter covers the central pseudorapidity range ($|\eta| < 1.7$). The endcap and forward regions are instrumented with LAr calorimeters for both the EM and hadronic energy measurements up to $|\eta| = 4.9$. The muon spectrometer surrounds the calorimeters and features three large air-core toroidal superconducting magnet systems with eight coils each. The field integral of the toroids ranges between 2.0 and 6.0 Tm across most of the detector. The muon spectrometer includes a system of precision tracking chambers up to $|\eta| = 2.7$ and fast detectors for triggering up to $|\eta| = 2.4$. A two-level trigger system [28] is used to select events. The first-level trigger is implemented in hardware and uses a subset of the detector information to reduce the accepted rate to at most 100 kHz. This is followed by a software-based trigger level that reduces the accepted event rate to 1 kHz on average.

4 Data and Monte Carlo simulation

The data sample was collected by the ATLAS detector during the pp collision running of the LHC at $\sqrt{s} = 13$ TeV in 2015 and 2016. Events were selected for the different channels with various triggers, as described in their respective papers [9–18]. Channels featuring charged or neutral leptons were selected with single or multiple electron and muon triggers with varyious p_{T} thresholds and isolation requirements, or with missing transverse momentum triggers with varying thresholds. A high-p_{T} jet trigger was used in the fully hadronic channels. After requiring that the data were collected during stable beam conditions and with a functional detector, the integrated luminosity amounts to 36.1 fb^{-1}.

The interpretation in the combined channels relies on MC simulation to model the shape and normalization of the signals described in Section 2. Signal events for the HVT and bulk RS models were generated with MadGraph5_aMC@NLO v2.2.2 [29] at leading order (LO) using the NNPDF23LO parton distribution function (PDF) set [30]. For the production of resonances in the HVT model, both the DY and VBF mechanisms were simulated, whereas for the bulk RS model, G_{KK} resonances were produced via the ggF and DY mechanisms. In the case of the heavy scalar model, signal events were generated at next-to-leading order (NLO) via the ggF and VBF mechanisms with Powheg-Box v1 [31, 32] and the CT10 PDF set [33]. The ggF/DY and VBF processes were simulated as independent MC samples. For all signal models and production mechanisms, the generated events were interfaced to Pythia v8.186 [34] for parton showering, hadronization, and the underlying event. This interface relied on the A14 set of tuned parameters [35] for events generated with MadGraph5_aMC@NLO at LO and the AZNLO set of tuned parameters [36] for events generated with Powheg-Box at NLO. Interference between the signal events and SM processes was not taken into account as the results for the bosonic channels are expected to change negligibly for the models considered since they predict narrow resonances. The particular case of $\ell\nu$ and $\ell\ell$ channels is discussed in Section 6. Examples of generator-level signal mass distributions are shown in Figure 2.

Simulated background event samples are used to derive the main background estimates in the case of analyses in the $\ell\nu$, $\ell\ell$, $\ell\nu\ell\ell$, and $\ell\ell\ell\ell$ channels, and to extrapolate backgrounds from control regions in the analysis of the other channels. In other cases, the data are used to extract the normalization and/or shape of the background distributions. Although the production of background MC samples differed somewhat depending on the specific analysis, most MC samples were produced as follows. Diboson (WW, WZ, ZZ) events were generated with Sherpa [37] or Powheg-Box; W+jets and Z+jets events were generated with Sherpa for up to two partons at NLO and up to four partons at LO using the OpenLoops [38] and Comix [39] programs, respectively. The production of top-quark pairs and single top quarks was performed at NLO with Powheg-Box. For the $\ell\nu$ and $\ell\ell$ channels, the dominant DY background was

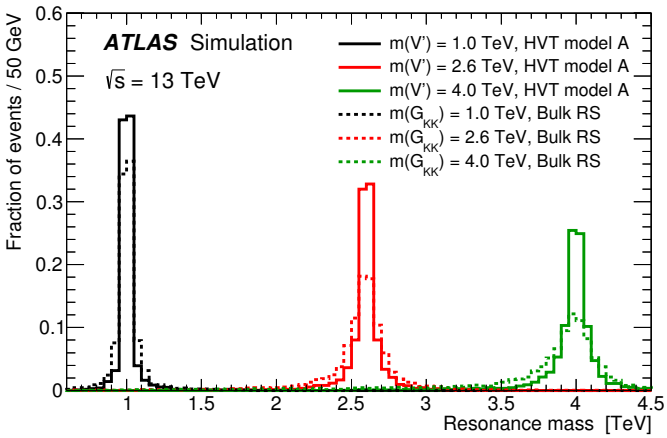

Figure 2: Generator-level mass distributions for HVT model A and the bulk RS signal model at resonance masses of 1.0, 2.6, and 4.0 TeV. The histograms are normalized to an area equal to unity.

modeled using POWHEG-BOX with next-to-next-to-leading-order QCD and NLO electroweak corrections. More specific details can be found in the papers for each analysis.

For all MC samples, except those produced with SHERPA, b-hadron and c-hadron decays were performed with EVTGEN v1.2.0 [40]. The production of the simulated event samples included the effect of multiple pp interactions per bunch crossing, as well as the effect on the detector response due to interactions from bunch crossings before or after the one containing the hard interaction. These effects are collectively referred to as "pileup." The simulation of pileup collisions was performed with PYTHIA 8 and tuned to reproduce the average of 23 pileup interactions observed in the data in addition to the hard-scatter interaction. Most of the MC samples were processed through a detailed simulation of the detector response with GEANT 4 [41, 42]. A small subset of MC samples were processed with a fast parameterization of the calorimeter response [43] while the response for the other detector components used GEANT 4. In all cases, events were reconstructed with the same software as was used for the data.

5 Event reconstruction

The event selection discussed in Section 6 relies on the reconstruction of electrons, muons, jets, and missing transverse momentum (with magnitude $E_{\mathrm{T}}^{\mathrm{miss}}$). Although the requirements vary for the different channels, the general algorithms are introduced below. The small differences between the efficiencies measured in data and MC simulation are corrected for by applying scale factors to the MC simulation so that it matches the data.

Measurements in the inner detector are used to reconstruct tracks from charged particles. The resulting tracks are then used to reconstruct collision vertices from pp interactions along the beam axis as well as vertices from the decays of b- and c-hadrons that are displaced from that axis. Out of the multiple collision vertices in each bunch crossing, a primary vertex is selected as the vertex with the largest $\sum p_{\mathrm{T}}^2$, where the sum is over all tracks with transverse momentum $p_{\mathrm{T}} > 0.4$ GeV which are associated with the vertex. Tracks associated with the primary vertex are identified as electrons or muons if they satisfy a set of criteria. Electrons are identified as tracks matching energy clusters in the electromagnetic calorimeter with

energy deposition consistent with that of an electromagnetic shower [44]. In addition, electron candidates must satisfy a set of isolation criteria [44]. Different tightness levels of identification and isolation are used depending on the needs of each analysis. Muons are identified by matching inner detector tracks to full tracks or track segments reconstructed in the muon spectrometer. Identification and isolation criteria that are specific to different tightness levels are detailed in Ref. [45].

Jets are reconstructed from clusters of energy deposits in calorimeter cells [46] with the anti-k_t clustering algorithm [47] implemented in FastJet [48]. To remove jets reconstructed from pileup, jet-vertex-tagging (JVT) is applied to jets with $p_{\mathrm{T}} < 60$ GeV and $|\eta| < 2.4$ [49]. Jets built using a radius parameter R equal to 0.4 are referred to as "small-R" jets and those built using R equal to 1.0 are referred to as "large-R" jets. A pair of small-R jets may be used to reconstruct $V \to qq$ decays at sufficiently small V momentum where they can be resolved, but a single large-R jet is used at higher momentum when the two small-R jets merge due to the high Lorentz boost. Small-R jets are built from clusters calibrated at the EM scale [50] while large-R jets are built from clusters calibrated at the local hadronic scale [51]. The latter jets are trimmed to minimize the impact of pileup and to improve their energy and mass resolution by reclustering the constituents of each jet with the k_t algorithm [52] into smaller $R = 0.2$ subjets and removing those subjets with $p_{\mathrm{T}}^{\mathrm{subjet}} / p_{\mathrm{T}}^{\mathrm{jet}} < 0.05$, where $p_{\mathrm{T}}^{\mathrm{subjet}}$ and $p_{\mathrm{T}}^{\mathrm{jet}}$ are the transverse momenta of the subjet and original jet, respectively. Calibration of the trimmed jet p_{T} and mass is described in Ref. [53].

Jets containing b-hadron decay products are tagged with a multivariate algorithm that exploits the presence of large-impact-parameter tracks and displaced vertices from b-hadron decays [54, 55]. Large-R jets are tagged as consistent with hadronic decays of W or Z bosons based on the mass (the mass window varies with jet p_T) and substructure of the jet [53, 56]. The latter exploits the two-body kinematics of high-p_{T} $V \to qq$ decays as measured by the variable D_2, which is defined as a ratio of two-point to three-point energy correlation functions that are based on the energies of, and pairwise angular distances between, the jet's constituents [56, 57]. Likewise, large-R jets may also be tagged as originating from $H \to bb$ decays by requiring the jet mass to be consistent with that of the Higgs boson (75–145 GeV) and the presence of two or more $R = 0.2$ jets built from tracks associated with the large-R jet, at least one of which must satisfy b-tagging requirements.

The magnitude of the event's missing transverse momentum is computed from the vectorial sum of the transverse momenta of calibrated electrons, muons, and small-R jets in the event [58]. The $E_{\mathrm{T}}^{\mathrm{miss}}$ value is corrected for the soft term, which consists of tracks associated with the primary vertex but not associated with electrons, muons, taus leptons, or small-R jets.

6 Event selection

The event selection and background estimation for the different analyses are briefly presented here. A full description is available in Refs. [9–18]. A list of the channels that are input to the combination is provided in Table 3 along with their experimental signatures. Care was taken in defining each of the signatures to achieve orthogonality between the different channels. The channels are broadly separated into three categories, depending on the targeted decay state of the intermediate resonance: a vector-boson pair (VV), a W or Z boson with an associated Higgs boson (VH), and a pair of leptons (not involving intermediate bosons). Within the VV category, there are three subcategories: fully hadronic, semileptonic, and fully leptonic. In the semileptonic and fully leptonic subcategories, the searches are further split into optimized selections for ggF/DY and VBF production (only the ggF/DY signature is indicated in Table 3). The VBF-enriched selections are made orthogonal to the ggF/DY selections by requiring the presence of

Table 3: Summary of analysis channels, diboson states they are sensitive to, and their experimental signatures. The selection reflects requirements specific to each channel. Additional jets (not included in the "Jets" column) are required to define VBF categories. The notation "j" represents small-R jets and "J" represents large-R jets. Leptons are either electrons or muons. A veto is imposed on $E_{\mathrm{T}}^{\mathrm{miss}}$ in some channels to guarantee orthogonality between final-state channels. The symbol "–" signifies that no requirement is imposed on a given signature.

Channel	Diboson state	Selection				VBF cat.	Reference
		Leptons	$E_{\mathrm{T}}^{\mathrm{miss}}$	Jets	b-tags		
$qqqq$	$WW/WZ/ZZ$	0	veto	2J	–	–	[9]
$\nu\nu qq$	WZ/ZZ	0	yes	1J	–	yes	[13]
$\ell\nu qq$	WW/WZ	$1e, 1\mu$	yes	2j, 1J	–	yes	[10]
$\ell\ell qq$	WZ/ZZ	$2e, 2\mu$	–	2j, 1J	–	yes	[13]
$\ell\ell\nu\nu$	ZZ	$2e, 2\mu$	yes	–	0	yes	[14]
$\ell\nu\ell\nu$	WW	$1e$+1μ	yes	–	0	yes	[12]
$\ell\nu\ell\ell$	WZ	$3e$, $2e$+1μ, $1e$+2μ, 3μ	yes	–	0	yes	[11]
$\ell\ell\ell\ell$	ZZ	$4e$, $2e$+2μ, 4μ	–	–	–	yes	[14]
$qqbb$	WH/ZH	0	veto	2J	1, 2	–	[15]
$\nu\nu bb$	ZH	0	yes	2j, 1J	1, 2	–	[16]
$\ell\nu bb$	WH	$1e, 1\mu$	yes	2j, 1J	1, 2	–	[16]
$\ell\ell bb$	ZH	$2e, 2\mu$	veto	2j, 1J	1, 2	–	[16]
$\ell\nu$	–	$1e, 1\mu$	yes	–	–	–	[17]
$\ell\ell$	–	$2e, 2\mu$	–	–	–	–	[18]

additional small-R jets, of which the two with highest p_{T} must have large η separation and high invariant mass. For the majority of the searches the discriminating variable is the invariant mass of the $VV/VH/\ell\ell$ candidates, except those which involve two neutrinos (or the $W' \to \ell\nu$ final state) where the transverse mass of the final-state particles is used.

Many of the searches involving charged leptons are affected by events with lepton candidates that originate from jets misidentified as leptons or with non-prompt leptons that originate from hadron decays. This background source is referred to as the "fake-lepton" background and is estimated using data-driven techniques. Events with fake leptons may arise from a variety of different processes including multijet, W/Z+jets, and $t\bar{t}$ production. Other background sources are estimated using MC simulation, with constraints sometimes extracted from control regions in the data.

The fully hadronic VV final state benefits from the largest branching fraction amongst the possible final states, but suffers from a large background contamination from the production of multijet events. However, this contamination can be mitigated in the regime of TeV-scale resonances with jet substructure techniques as described in Section 5. The background prediction is obtained with a fit to the invariant mass distribution of the two highest-p_{T} large-R jets in the event. This channel explores the mass range between 1.1 and 5.0 TeV and is particularly sensitive at high resonance mass.

The semileptonic VV analyses require either two small-R jets or one large-R jet, for the resolved and merged regimes respectively, in addition to zero, one, or two leptons, with significant $E_{\mathrm{T}}^{\mathrm{miss}}$ required in all channels except $\ell\ell qq$. Control regions are used to derive the background estimate, and separate signal regions are defined so as to be sensitive to the different production mechanisms, i.e. ggF/DY or VBF

production. The background in the $\nu\nu qq$ channel has large contributions from W/Z+jets and $t\bar{t}$ events. The background in the $\ell\nu qq$ channel is dominated by W+jets and $t\bar{t}$ events, while the background in the $\ell\ell qq$ channel is dominated by Z+jets events. These channels are used in the mass range from 0.3 to 5.0 TeV and are particularly sensitive in the mid- to high-mass range.

For the fully leptonic VV final states, different selection categories are defined for each channel to optimize the sensitivity to DY, ggF, and VBF production. In the $\ell\nu\ell\nu$ channel, two VBF categories are defined with $N_{\text{jet}} = 1$ and $N_{\text{jet}} \geq 2$, with additional criteria on the jet η and separation between the leptons and jets to minimize contamination from the ggF signal. A third category for ggF production is further defined as those events that fail to enter the two VBF categories, while satisfying the other base criteria, ensuring orthogonality. The major backgrounds in the $\ell\nu\ell\nu$ channel come from WW and $t\bar{t}$ production. This channel is used in the mass range 0.5–5.0 TeV (0.5–1.0 TeV) for ggF (VBF) production with particular sensitivity at lower mass. For the $\ell\nu\ell\ell$ channel, two categories are defined to discriminate between DY and VBF production mechanisms. The dominant background in the $\ell\nu\ell\ell$ channel is the contribution from WZ production, and this channel has particular sensitivity in the mass range 0.3–3.0 TeV (0.3–2.0 TeV) for DY (VBF) production. The $\ell\ell\ell\ell$ channel considers all combinations of electron and muon pairs, with ZZ production as the main background contribution. This channel provides good sensitivity for resonance masses below 1 TeV, and covers the range of 0.2–2.0 TeV. Finally, the $\ell\ell\nu\nu$ channel requires exactly two same-flavor and oppositely charged electrons or muons, with the dilepton invariant mass required to be within the Z-mass region. This channel has four signal categories: two for ggF and two for VBF production, divided according to the flavor of the leptons they contain. This channel covers the resonance mass range of 0.3–2.0 TeV, with a particular sensitivity at low mass, between 0.5 TeV and 1.0 TeV.

The fully hadronic VH analysis focuses on resonance masses above 1 TeV, with highly boosted V bosons and Higgs bosons that are likely to be highly collimated and merged into a single large-R jet. The analysis uses dedicated boosted-boson tagging and only considers the merged regime, requiring at least two large-R jets with high p_{T}, with a veto on any event that contains a lepton candidate. The main background in this search comes from multijet processes.

The semileptonic VH analyses focus on the resonance mass region above 0.5 TeV. Regimes in which the V or H boson decay constituents are separated enough to be considered resolved and those in which they are merged are both considered in separate categories, with priority given to the resolved analysis, and the remaining events recycled into the merged analysis. The semileptonic searches are split into three channels depending on the number of charged leptons: $\nu\nu bb$, $\ell\nu bb$, and $\ell\ell bb$.

The $\ell\nu$ and $\ell\ell$ final states have a high sensitivity due to their very clean signature, with good lepton energy resolution and relatively low background. The dominant background in these channels comes from the irreducible charged-current (CC) and neutral-current (NC) DY processes for the $\ell\nu$ and $\ell\ell$ channels, respectively. These searches are sensitive across a wide range of resonance masses from 0.2 to 5.5 TeV.

For a number of the signatures there is interference between the signal and the SM background. For some channels such as the hadronic and semileptonic diboson decay channels, the impact of interference is expected to be negligible because the SM diboson background is small. Moreover, multijet event production is depleted in $qqqq$ states and thus the interference with the fully hadronic decay channel is reduced. For the fully leptonic diboson decay channels this background is not negligible but the role of interference, which increases with the heavy resonance width, is small for widths less than 15% of the resonance pole mass. Since only narrow resonances are considered, the impact of interference is neglected. Finally, for the leptonic channels ($\ell\nu$, $\ell\ell$) the interference can play an important role as the dominant background is the irreducible DY process which interferes with the HVT signal, and thus to minimize

the effects of interference the $\ell\nu$ transverse mass is required to satisfy $|m_{\mathrm{T}} - m_{\mathrm{pole}}| < \sqrt{64\ \mathrm{GeV} \times m_{\mathrm{pole}}}$ in the $\ell\nu$ channel, where m_{pole} corresponds to the W' pole mass. Likewise, the $\ell\ell$ mass is required to satisfy $|m_{\ell\ell} - m_{\mathrm{pole}}| < \sqrt{25\ \mathrm{GeV} \times m_{\mathrm{pole}}}$ in the $\ell\ell$ channel with m_{pole} the Z' pole mass. The mass window requirement results in the difference between the theoretical cross section with and without interference being less than 15% throughout the coupling plane.

Possible overlaps among the different searches in the combination are considered to ensure orthogonality. The first step is to determine the orthogonality of the selection criteria used in the various analyses, which is summarized in Table 3. One of the criteria that cleanly provides orthogonality is the requirement on the lepton multiplicity in the selected events, ranging from zero to four leptons. Further orthogonality is achieved with additional selection criteria for the jets and $E_{\mathrm{T}}^{\mathrm{miss}}$ in the events. In particular, a veto is applied to events with large $E_{\mathrm{T}}^{\mathrm{miss}}$ value in the $qqqq$, $qqbb$, and $\ell\ell bb$ channels. For the combination of VV and VH channels (and also with the leptonic channels), events are further removed from the VH analysis if they are in overlapping parts of the signal region and have a Higgs boson candidate mass close to the W/Z mass. This has the effect of improving the VH sensitivity in the combination above 1 TeV by 10–15% because the original VH semileptonic analyses were optimized for resonances with a mass below 1 TeV. Only a negligible number of events that overlap between channels remain.

7 Systematic uncertainties

The various sources of experimental and theoretical systematic uncertainty are assessed as a function of the discriminating variable in each of the search channels in the combination. These uncertainties are derived for both the signal and background estimates where relevant, and are treated as correlated or uncorrelated between the signal and background in the various channels, as appropriate. The systematic uncertainties estimated to have a non-negligible impact on the expected cross-section limit are used as nuisance parameters in the statistical interpretation, as described in Section 8. This section describes the systematic uncertainties for all channels in the combination, and applies to the various signal scenarios in Table 2. A full description of the evaluation of systematic uncertainties is provided in the original publications for each of the analyses. What follows is a qualitative discussion.

The experimental systematic uncertainties related to charged leptons, such as the efficiencies due to triggering, reconstruction, identification, and isolation, as well as the lepton energy scale and resolution, are evaluated using $Z \to \ell\ell$ decays and then extrapolated to higher energies. These uncertainties are correlated between leptons of the same flavor across all channels in the combination, and between the signal and the background estimates. The systematic uncertainties for each of the channels featuring charged leptons are summarized in Table 4 including the assumed correlation between channels.

The experimental systematic uncertainties due to the missing transverse momentum are summarized in Table 5. These relate to the $E_{\mathrm{T}}^{\mathrm{miss}}$ trigger, as well as the $E_{\mathrm{T}}^{\mathrm{miss}}$ scale and resolution, which are estimated in control regions using the data.

The small-R jet uncertainties are relevant for most of the channels in the combination, including those with leptonic final states that contain at least one neutrino, due to the impact of those uncertainties on the $E_{\mathrm{T}}^{\mathrm{miss}}$ measurement. The uncertainties in the jet energy scale and resolution are derived by comparing the response between the data and the simulation in various kinematic regions and event topologies. Additional contributions to this uncertainty come from the dependence on the pileup activity and on the flavor composition of the jets, as well as the punch-through of the energy from the calorimeter into the

muon spectrometer. An uncertainty in the efficiency for jets to satisfy the JVT requirements is assessed. The small-R jet uncertainties are summarized in Table 6. For large-R jets, the uncertainties in the energy, mass, and D_2 scales are estimated by comparing the ratio of calorimeter-based to track-based jet p_{T} measurements in dijet events between the data and the simulation. The uncertainties in the jet mass resolution and jet energy resolution, as well as D_2 are assessed by applying additional smearing of the jet observables according to the uncertainty in their resolution measurements. A summary of the large-R jet systematic uncertainties is provided in Table 7.

The flavor-tagging uncertainty is evaluated by varying the data-to-MC corrections in various kinematic regions, based on the measured tagging efficiency and mistag rates. These variations are applied separately to b-hadron jets, c-hadron jets, and light (quark or gluon) jets, leading to three uncorrelated systematic uncertainties. An additional uncertainty is included due to the extrapolation for the jets with p_{T} beyond the kinematic reach of the data calibration. The flavor-tagging uncertainties are summarized in Table 8.

The theoretical uncertainties are split among the various backgrounds, which play greater or lesser roles in each of the search channels, depending on the composition of backgrounds in a given channel. The dominant background in the $\ell\nu$ and $\ell\ell$ channels is from the CC and NC DY processes, respectively. In these channels, theoretical uncertainties arise from PDFs and electroweak corrections. The PDF uncertainties are divided into PDF eigenvector variations, choice of the nominal PDF set (CT14NNLO [59]) from a number of different PDF sets, as well as the choice of PDF renormalization and factorization scales, and α_{S}. In the case of the $\ell\ell$ channel, an additional uncertainty due to photon-induced corrections to the NC DY process is also assessed. Similar sources of uncertainty are assessed and included where relevant for other backgrounds such as: top-quark, diboson, V+jets, as well as for the multijet background, when an MC-based estimation is used. Specifically, when "cross section" uncertainties are mentioned for these backgrounds they refer to cross-section calculations, while "modeling" refers to event generator and parton shower comparisons, and "extrapolation" refers to the background being extrapolated from a control region to a higher mass region. One exception is the multijet-modeling systematic uncertainty for channels that include leptons, such as $\ell\nu$ and $\ell\ell$. In these cases the systematic uncertainty includes variations of the data-driven methodology used to derive the fake-lepton background estimate and its subsequent extrapolation to higher masses. All uncertainties are summarized in Table 9. Theoretical uncertainties that affect the acceptance of the signal are also assessed, such as initial- and final-state radiation, PDF variation, and PDF choice. These generally have a negligible impact on the result, but are included where relevant in the statistical interpretation.

All channels include an uncertainty in the integrated luminosity of 3.2% derived following a methodology similar to that detailed in Ref. [60]. This uncertainty is taken to be correlated across the channels and between signal and background. The uncertainty due to pileup is also considered when it does not have a negligible impact on the analysis, to cover the difference between the ratios of predicted and measured inelastic cross-section values.

For most of the VV and VH analyses, MC-modeling systematic uncertainties play the dominant role in the theoretical uncertainty, while for the leptonic channels, the PDF variation and PDF choice are by far the most dominant. For the experimental systematic uncertainties, analyses selecting jets are most sensitive to systematic uncertainties in the modeling of large-R jets, while the leptonic channels are affected mostly by the uncertainty in the muon reconstruction efficiency and electron isolation efficiency.

Table 4: Lepton systematic uncertainties. The abbreviations "S" and "B" stand for signal and background, respectively. Each uncertainty is considered as correlated between the channels listed.

Source	$\ell\nu qq$	$\ell\ell qq$	$\ell\ell\nu\nu$	$\ell\nu\ell\nu$	$\ell\nu\ell\ell$	$\ell\ell\ell\ell$	$\ell\nu bb$	$\ell\ell bb$	$\ell\nu$	$\ell\ell$
Electron trigger	S+B	S+B	S+B	S+B	negl.	S+B	S+B	S+B	negl.	negl.
Electron reconstruction	S+B	S+B	S+B	S+B	S+B	S+B	S+B	S+B	negl.	negl.
Electron identification	S+B	S+B	S+B	S+B	S+B	S+B	S+B	S+B	negl.	S+B
Electron isolation	S+B	S+B	S+B	S+B	S+B	S+B	S+B	S+B	negl.	S+B
Electron energy scale	S+B	S+B	S+B	S+B	S+B	S+B	S+B	S+B	S+B	S+B
Electron energy resolution	S+B	S+B	S+B	S+B	S+B	S+B	S+B	S+B	negl.	S+B
Muon trigger	S+B	S+B	S+B	S+B	negl.	S+B	S+B	S+B	S+B	negl.
Muon reconstruction	S+B	S+B	S+B	S+B	S+B	S+B	S+B	S+B	S+B	S+B
Muon isolation	S+B	S+B	S+B	S+B	S+B	S+B	S+B	S+B	negl.	S+B
Muon momentum scale	S+B	S+B	S+B	S+B	S+B	S+B	S+B	S+B	negl.	negl.
Muon momentum resolution	S+B	S+B	S+B	S+B	S+B	S+B	S+B	S+B	S+B	S+B

Table 5: $E_{\mathrm{T}}^{\mathrm{miss}}$ systematic uncertainties. The abbreviations "S" and "B" stand for signal and background, respectively, while "–" denotes uncertainties that are not applicable. Each uncertainty is considered as correlated between the channels listed.

Source	$\nu\nu qq$	$\ell\nu qq$	$\ell\ell\nu\nu$	$\ell\nu\ell\nu$	$\ell\nu\ell\ell$	$\nu\nu bb$	$\ell\nu bb$	$\ell\nu$
$E_{\mathrm{T}}^{\mathrm{miss}}$ trigger	S+B	S+B	S+B	–	–	S+B	S+B	–
$E_{\mathrm{T}}^{\mathrm{miss}}$ soft-term scale	S+B	S+B	S+B	S+B	S+B	S+B	S+B	S+B
$E_{\mathrm{T}}^{\mathrm{miss}}$ soft-term resolution	S+B	S+B	S+B	S+B	S+B	S+B	S+B	S+B

Table 6: Small-R jet systematic uncertainties. The abbreviations "S" and "B" stand for signal and background, respectively. Each uncertainty is considered as correlated between the channels listed.

Source	$\nu\nu qq$	$\ell\nu qq$	$\ell\ell qq$	$\ell\ell\nu\nu$	$\ell\nu\ell\nu$	$\ell\nu\ell\ell$	$qqbb$	$\nu\nu bb$	$\ell\nu bb$	$\ell\nu$
Small-R jet energy scale	S+B	S+B	S+B	S+B	S+B	S+B	S+B	S+B	S+B	S+B
Small-R jet energy resolution	S+B	S+B	S+B	S+B	S+B	S+B	S+B	S+B	S+B	S+B
Small-R jet flavor	S+B	S+B	S+B	S+B	S+B	negl.	S+B	S+B	S+B	S+B
Small-R jet pileup	S+B	S+B	S+B	S+B	S+B	negl.	S+B	S+B	S+B	S+B
Small-R jet punch-through	S+B	S+B	S+B	S+B	S+B	negl.	S+B	S+B	S+B	S+B
Small-R jet JVT	S+B	S+B	S+B	S+B	S+B	S+B	S+B	S+B	S+B	S+B

Table 7: Large-R jet systematic uncertainties. The abbreviations "S" and "B" stand for signal and background, respectively. Each uncertainty is considered as correlated between the channels listed.

Source	$qqqq$	$\nu\nu qq$	$\ell\nu qq$	$\ell\ell qq$	$qqbb$	$\nu\nu bb$	$\ell\nu bb$	$\ell\ell bb$
Large-R jet D_2 scale	S	S+B	S+B	S+B	S+B	S+B	S+B	S+B
Large-R jet D_2 resolution	S	S+B	S+B	S+B	S+B	S+B	S+B	S+B
Large-R jet scale	S	S+B	S+B	S+B	S+B	S+B	S+B	S+B
Large-R jet resolution	S	S+B	S+B	S+B	S+B	S+B	S+B	S+B
Large-R jet mass scale	S	S+B	S+B	S+B	S+B	S+B	S+B	S+B
Large-R jet mass resolution	S	S+B	S+B	S+B	S+B	S+B	S+B	S+B

Table 8: Flavor-tagging systematic uncertainties. The abbreviations "S" and "B" stand for signal and background, respectively. Each uncertainty is considered as correlated between the channels listed.

Source	$\nu\nu qq$	$\ell\nu qq$	$\ell\ell qq$	$\ell\ell\nu\nu$	$\ell\nu\ell\nu$	$\ell\nu\ell\ell$	$qqbb$	$\nu\nu bb$	$\ell\nu bb$	$\ell\ell bb$
b-tagging	S+B	S+B	S+B	B	B	B	S+B	S+B	S+B	S+B
c-tagging	S+B	S+B	S+B	B	B	B	S+B	S+B	S+B	S+B
Light-q tagging	S+B	S+B	S+B	B	B	B	S+B	S+B	S+B	S+B
Tagging extrapolation	S+B	S+B	S+B	B	B	B	S+B	S+B	S+B	S+B

Table 9: Theoretical systematic uncertainties. The abbreviation "B" stands for background, while "–" denotes uncertainties that are not applicable, "negl." denotes uncertainties that are negligible, and "Corr" marks whether the uncertainty is correlated between the channels listed. The abbreviation "F" means that this parameter was left to float in the background control region for that channel. The systematic uncertainties in the background modeling for the fully hadronic analysis $qqqq$ are embedded in the fit function used to model the background.

Source	Corr	$\nu\nu qq$	$\ell\nu qq$	$\ell\ell qq$	$\ell\ell\nu\nu$	$\ell\nu\ell\nu$	$\ell\nu\ell\ell$	$qqbb$	$\nu\nu bb$	$\ell\nu bb$	$\ell\ell bb$	$\ell\nu$	$\ell\ell$
DY PDF variation	Yes	–	–	–	–	–	–	–	–	–	–	B	B
DY PDF choice	Yes	–	–	–	–	–	–	–	–	–	–	B	B
DY PDF scale	Yes	–	–	–	–	–	–	–	–	–	–	negl.	B
DY α_S	Yes	–	–	–	–	–	–	–	–	–	–	B	B
DY EW corrections	Yes	–	–	–	–	–	–	–	–	–	–	B	B
DY photon-induced	Yes	–	–	–	–	–	–	–	–	–	–	–	B
Top cross section	No	B	F	F	B	B	–	B	B	B	B	B	negl.
Top extrapolation	No	–	–	–	–	–	–	–	–	–	–	B	–
Top modeling	No	B	B	B	B	B	–	–	B	B	B	negl.	negl.
Diboson cross section	No	B	B	B	B	B	–	B	B	B	B	negl.	negl.
Diboson extrapolation	No	–	–	–	–	–	–	–	–	–	–	B	–
Multijet cross section	No	–	B	–	–	–	B	B	–	B	–	–	–
Multijet modeling	No	–	–	–	–	–	–	B	–	B	–	B	B
Z+jets cross section	No	F	B	F	–	–	–	–	B	B	B	–	–
Z+jets modeling	No	B	B	B	–	–	–	–	B	B	B	–	–
W+jets cross section	No	B	F	B	–	–	–	–	B	B	B	–	–
W+jets modeling	No	B	B	B	–	–	–	–	B	B	B	–	–

8 Statistical treatment

The combination of the individual channels proceeds with a simultaneous analysis of the signal discriminants across all of the channels. For each signal model being tested, only the channels sensitive to that hypothesis are included in the combination. The statistical treatment of the data is based on the RooFit [61], RooStats [62], and HistFactory [63] data modeling and handling toolkits. Results are calculated in two different signal parameterization paradigms, corresponding to one-dimensional upper limits on the cross section times branching fraction ($\sigma \times \mathcal{B}$) and two-dimensional limits on coupling strengths. The statistical treatment of each case is described here.

8.1 One-dimensional upper limits

In the case of one-dimensional upper limits on $\sigma \times \mathcal{B}$, the overall signal strength, μ, defined as a scale factor multiplying the cross section times branching fraction predicted by the signal hypothesis, is the parameter of interest. The analysis follows the frequentist approach with a test statistic based on the profile-likelihood ratio [64]. This test statistic ($\mathcal{T}$) is defined as twice the negative logarithm of the ratio of the conditional (fixed-μ) maximum likelihood to the unconditional maximum likelihood, each obtained from a fit to the data:

$$\mathcal{T} = -2 \ln \frac{L(\mu, \hat{\hat{\boldsymbol{\theta}}}(\mu))}{L(\hat{\mu}, \hat{\boldsymbol{\theta}}(\hat{\mu}))}, \tag{2}$$

where $\theta(\mu)$ represent the nuisance parameters. The latter are represented in the equation as their unconditional and conditional maximum-likelihood values, $\hat{\boldsymbol{\theta}}(\hat{\mu})$ and $\hat{\hat{\boldsymbol{\theta}}}(\mu)$. The fitted signal strength, $\hat{\mu}$, is bounded from below at zero.

The likelihood, L, is given by

$$L = \prod_c \prod_i \text{Pois}\left(n_{ci}^{\text{obs}} \,\middle|\, n_{ci}^{\text{sig}}(\mu, \vec{\theta}) + n_{ci}^{\text{bkg}}(\vec{\theta})\right) \prod_k f_k(\theta_k)\,,$$

where the index c represents the analysis channel, i represents the bin in the signal discriminant distribution, n^{obs} the observed number of events, n^{sig} the number of expected signal events, n^{bkg} the expected number of background events, $\vec{\theta}$ the vector of nuisance parameters, and $\text{Pois}(x|y)$ is the Poisson probability to observe x events when y are predicted.

The effect of a systematic uncertainty k on the binned likelihood is modeled with an associated nuisance parameter, θ_k, constrained with a corresponding probability density function $f_k(\theta_k)$. In this manner, correlated effects across the different channels are modeled by the use of a common nuisance parameter and its corresponding probability density function. The $f_k(\theta_k)$ terms are Poisson-distributed for bin-by-bin MC statistical uncertainties, and Gaussian-distributed for all other terms.

Given the large number of search channels included in the likelihood, the sampling distribution of the profile-likelihood test statistic is assumed to follow the chi-squared (χ^2) distribution and thus asymptotic formulae for the evolution of the likelihood as a function of signal strength (μ) are used [64]. In certain instances, such as high-mass tails of resonant mass distributions, the asymptotic approximation is expected

to be less reliable. In these cases, MC trials are used to assess its accuracy. This approximation is found to lead to $\sigma \times \mathcal{B}$ limits that are stronger than those obtained with MC trials. The effect is largest in the case of the lepton–antilepton combination for which it increases linearly with resonance mass from approximately 20% at 2 TeV to 55% at 5 TeV. In the context of HVT model A, the impact of using the asymptotic approximation in the limit setting is at most 250 GeV on the mass limits, as obtained for the lepton-antilepton combination.

When evaluating limits in the HVT model with degenerate-mass W' and Z' production, each of the contributing signal processes is normalized to the $\sigma \times \mathcal{B}$ value predicted by HVT model A, thereby defining the relative ratios of $\sigma(pp \to W')/\sigma(pp \to Z')$, $\mathcal{B}(W' \to \ell\nu)/\mathcal{B}(W' \to WZ/WH)$ and $\mathcal{B}(Z' \to \ell\ell)/\mathcal{B}(Z' \to WW/ZH)$. The HVT model A benchmark makes a model-dependent assumption about these relative ratios, so the resulting upper limits cannot be directly interpreted as general limits on $\sigma \times \mathcal{B}$. Thus, the upper limits are presented as the ratio to the HVT model A prediction for $\sigma \times \mathcal{B}$, as each of the previously defined ratios are fixed to this benchmark prediction.

Upper limits on μ for the signal models being tested at the simulated resonance masses are evaluated at the 95% confidence level (CL) following the $\mathrm{CL_s}$ prescription [65]. Lower limits on the mass of new resonances in these models are obtained by finding the maximum resonance mass where the 95% CL upper limit on μ is less than or equal to unity. This mass is found by interpolating between the limits on μ at the simulated signal masses. The interpolation assumes monotonic and smooth behavior of the efficiencies for the signal and background processes, and that the impact of the variation of signal mass distributions between adjacent test masses is negligible.

8.2 Two-dimensional limits

When calculating one-dimensional upper limits on $\sigma \times \mathcal{B}$, each of the signal rate predictions from W' and Z' production is fixed to the ratio predicted by the benchmark models. To evaluate two-dimensional constraints on coupling strengths, the signal yields are parameterized with a set of coupling parameters ($\vec{g}$) which allow the relative proportions of each signal to vary independently. Thus, in the two-dimensional limit calculation, Eq. (2) is modified to allow the set of coupling parameters to be considered independently:

$$\mathcal{T}' = -2 \ln \frac{L(\vec{g}, \hat{\hat{\boldsymbol{\theta}}}(\vec{g}))}{L(\hat{\vec{g}}, \hat{\boldsymbol{\theta}}(\hat{\vec{g}}))}.$$

The coupling parameterization assumes that all signal production proceeds via quark–antiquark annihilation (proportional to g_q^2) and the signal decays are proportional to the square of the bosonic coupling (g_H) and leptonic coupling (g_ℓ) in the $V' \to VV/VH$ and $V' \to \ell\nu/\ell\ell$ final states, respectively.

Two coupling spaces are considered. The first coupling scenario makes the assumption of common fermionic couplings ($g_f = g_\ell = g_q$), and probes the $\{g_H, g_f\}$ plane. The second coupling scenario allows independent fermionic couplings, and probes the $\{g_q, g_\ell\}$ plane with either $g_H = 0$ or $g_H = -0.56$, where the latter takes the value predicted in the HVT model A benchmark. The 95% CL limit contours in each coupling space are determined using $\mathcal{T}'$ by normalizing signal rates to the $\sigma \times \mathcal{B}$ predictions of the HVT model for the specified values of $\vec{g}$ at a given point in the space and calculating the value of $\mathrm{CL_s}$ for that point. Upper limits on coupling parameters are thus defined by contours of constant $\mathrm{CL_s}$ in each coupling space considered.

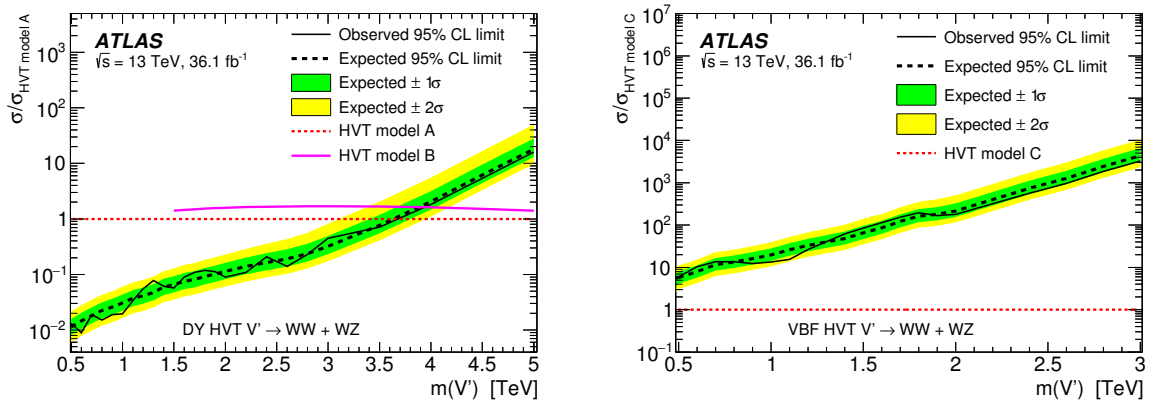

(a) (b)

Figure 3: Observed and expected 95% CL upper limits on the V' cross section times branching fraction to WW or WZ for the HVT benchmark model, relative to the cross section times branching fraction for HVT models A or C, as applicable. Results are shown for (a) DY and (b) VBF production mechanisms. The model predictions are also shown.

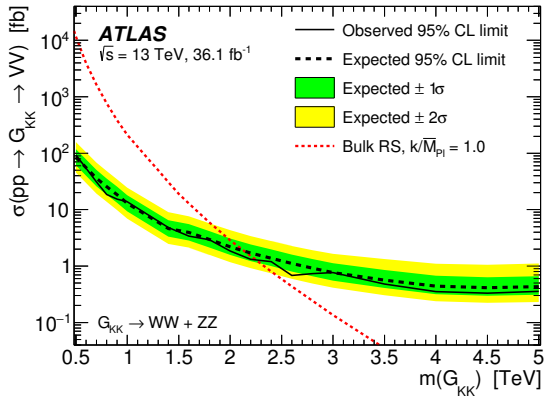

Figure 4: Observed and expected 95% CL upper limits on the G_{KK} cross section times branching fraction to WW or ZZ for the bulk RS model with $k/\overline{M}_{\mathrm{Pl}} = 1$. The model prediction is also shown.

9 Results

The methodology described in the previous section is used to statistically combine various channels for the different signal models listed in Table 2. The largest local excess is observed in the VBF Scalar (WW+ZZ) search for a mass of 1.6 TeV, with a significance of 2.9 σ. Limits are set on the signal parameters of interest.

For the VV combination, the HVT, bulk RS, and scalar models are all considered. Figure 3 shows the $\sigma \times \mathcal{B}$ limit relative to the predicted $\sigma \times \mathcal{B}$ for the combination of $W' \to WZ$ and $Z' \to WW$ decays in the context of the HVT model for either DY or VBF production mechanisms. Cross-section limits obtained exclusively for the VBF production mechanism are useful for constraining models with small coupling between fermions and V' resonances. Figures 4 and 5 show the $\sigma \times \mathcal{B}$ limits for the combination of $G_{\mathrm{KK}} \to WW$ or ZZ and Scalar $\to WW$ or ZZ, respectively.

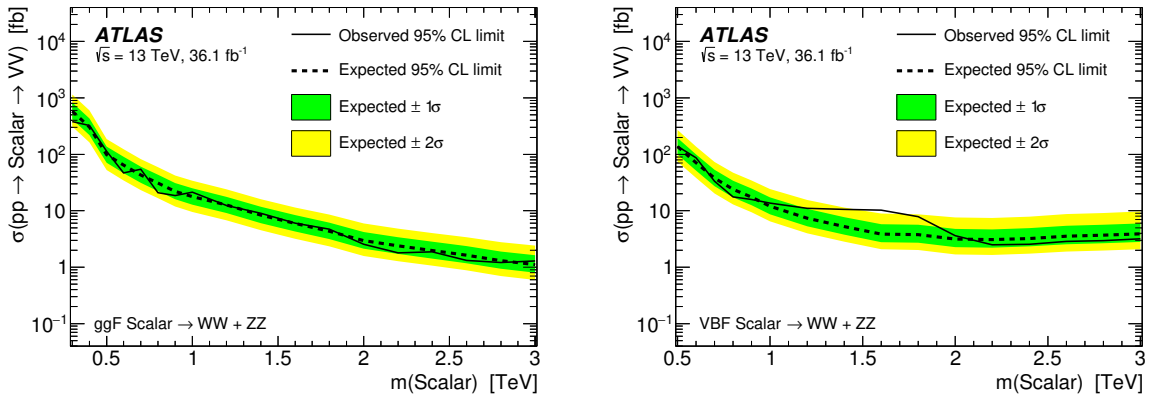

(a) (b)

Figure 5: Observed and expected 95% CL upper limits on the cross section times branching fraction to WW or ZZ for a scalar particle. Results are shown for (a) DY and (b) VBF production mechanisms.

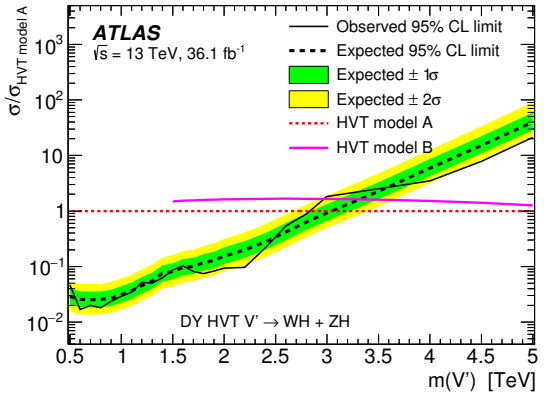

Figure 6: Observed and expected 95% CL upper limits on the V' cross section times branching fraction to WH or ZH for the HVT benchmark model, relative to the cross section times branching fraction for HVT model A. The model predictions are also shown.

For the combination of VH search channels, only the HVT benchmark models are considered. Figure 6 shows the $\sigma \times \mathcal{B}$ limits relative to the HVT model A cross section, for decays into WH and ZH combined.

The VV and VH channels are then combined, setting limits on $\sigma \times \mathcal{B}$ relative to the HVT model A prediction, as shown in Figure 7(a). For the leptonic channels ($W' \to \ell\nu$ and $Z' \to \ell\ell$) only HVT model A is considered as shown in Figure 7(b).

The channels are then further combined to set limits on HVT model A using not only VV and VH decay modes, but also $\ell\nu/\ell\ell$ decay modes. Figure 8 presents the resulting limits on $\sigma \times \mathcal{B}$ relative to the HVT model A prediction for W', Z', and V' production. Separate VV/VH and $\ell\nu/\ell\ell$ expected limits are shown in Figure 8(d). As the VV and VH analyses only usually consider V' masses up to 5 TeV, the acceptance is extrapolated to 5.5 TeV for the full combination.

Each of the channels presented here contributes uniquely to the search for heavy resonances, and the results obtained by their combination extend the reach beyond that of the individual searches. By using

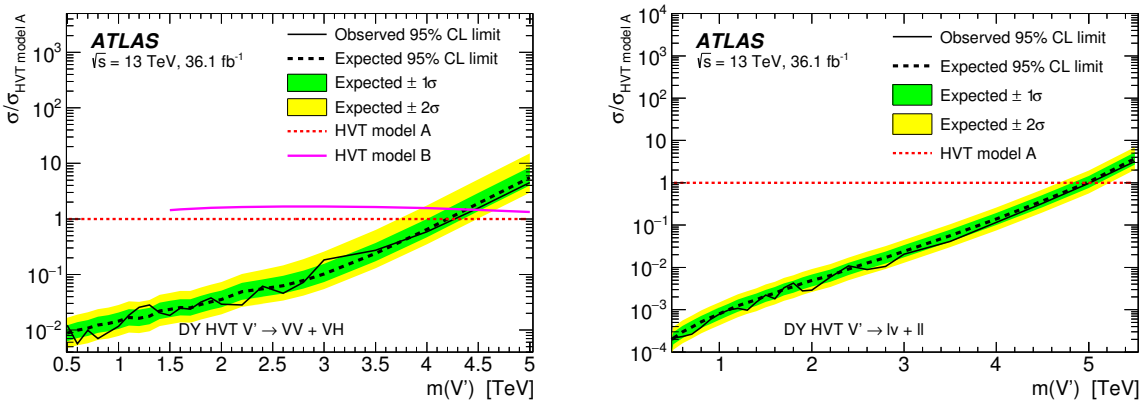

(a) (b)

Figure 7: Observed and expected 95% CL upper limits on the V' cross section times branching fraction to (a) VV/VH and (b) $\ell\nu/\ell\ell$ for the HVT benchmark model, relative to the cross section for HVT model A. The model predictions are also shown.

the HVT, bulk RS, and scalar benchmark models for comparison, the relative exclusion power of each search and their combinations can be compared. The intersection of the benchmark model predictions and the $\sigma \times \mathcal{B}$ upper limits yield lower limits on the resonance mass in each case. The observed and expected lower limits on the resonance mass are summarized in Table 10.

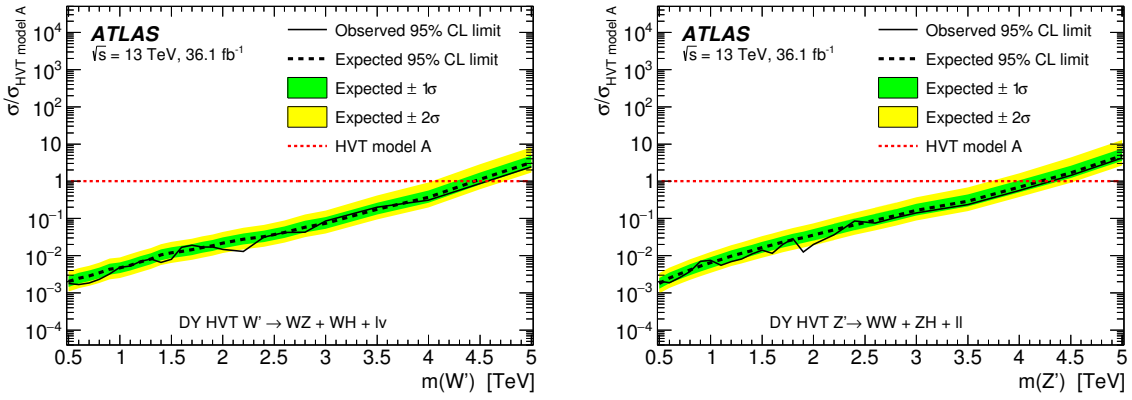

(a)

(b)

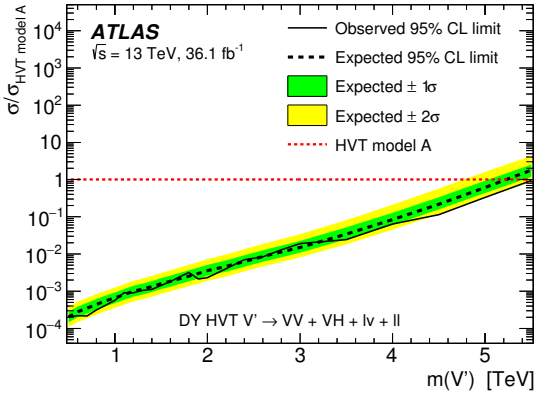

(c)

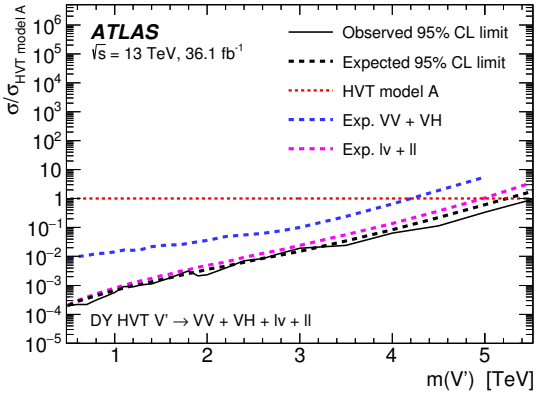

(d)

Figure 8: Observed and expected 95% CL upper limits on the V' cross section times branching fraction to VV, VH, and lepton–antilepton, relative to the prediction for HVT model A. Results are shown for (a) W', (b) Z', and (c) V' production; (d) shows expected limits for bosonic and leptonic decay modes. The model predictions are also shown.

Table 10: Observed and expected 95% CL lower limits on resonance mass for benchmark models in each of the combined searches.

Channel	Lower limits on resonance mass [TeV]					
	HVT model A		HVT model B		Bulk RS	
	Obs	Exp	Obs	Exp	Obs	Exp
WW	2.9	3.1	3.6	3.5	1.7	1.9
WZ	3.6	3.6	3.9	3.9	-	-
ZZ	-	-	-	-	1.5	1.7
VV	3.7	3.7	4.0	3.9	2.3	2.2
WH	2.6	2.8	2.8	3.1	-	-
ZH	2.7	2.5	2.8	2.8	-	-
VH	2.8	3.1	3.0	3.4	-	-
$\ell\nu$	4.6	4.6	-	-	-	-
$\ell\ell$	4.5	4.4	-	-	-	-
$\ell\nu/\ell\ell$	5.0	5.0	-	-	-	-
VV/VH	4.3	4.3	4.5	4.4	-	-
$VV/VH/\ell\nu/\ell\ell$	5.5	5.3	-	-	-	-

The search channels included here provide access to several coupling strengths of heavy resonances to SM particles as described by Eq. (1) in the context of the HVT model. Specifically, the data constrain the coupling strength to both the quarks and bosons in the VV and VH channels, whereas constraints are placed on both the quark and lepton couplings in the leptonic channels. These constraints are shown in Figures 9, 10, and 11, where the first and second include a shaded area denoting a region where the limits are not valid because resonances would have a width greater than 5% of their mass. This is a region where the resonance width would exceed the discriminating variable's resolution in the search, and the assumed narrow-width approximation breaks down. Figures 10 and 11 include constraints on heavy resonances with masses of 3, 4, and 5 TeV from precision electroweak (EW) measurements [66], which already exclude this aforementioned region for the relevant contours shown. The EW constraints are only overlaid on the final plots for each part of the combination.

The constraints from the VV, VH, and combined VV and VH channels are presented in Figure 9, showing the $\{g_H, g_f\}$ plane for each, as well as the $\{g_q, g_\ell\}$ plane for VV/VH. These constraints are strongest at large couplings for both g_f and g_H, but become weak as these couplings approach zero. This is because the resonance couplings to VV and VH tend to zero as the g_H coupling approaches zero, and production of the resonance also tends to zero as the g_f coupling approaches zero. The constraints in the $\{g_q, g_\ell\}$ plane shown in Figure 9(d) weaken at larger $|g_\ell|$ values due to an increase in the leptonic branching fraction and a corresponding decrease in the bosonic branching fraction.

Figure 10 presents the constraints from the $\ell\nu/\ell\ell$ channels in the $\{g_H, g_f\}$ plane, $\{g_q, g_\ell\}$ plane for g_H set to the value from HVT model A, and $\{g_q, g_\ell\}$ plane for g_H set to 0. In this last case the bosonic channels do not contribute because $g_H = 0$, meaning only the leptonic channels contribute. As the leptonic channels involve direct production of a V' resonance and subsequent decay, without intermediate bosons, the constraints remain strong even as g_H tends to zero, and in fact are strongest there due to the restriction of alternative decay modes. The constraints from these channels still weaken as the g_f coupling tends to zero though, as it does when g_ℓ and/or g_q tend to zero. These features demonstrate the complementarity between the VV/VH and $\ell\nu/\ell\ell$ decay modes.

The complementarity is further evidenced by the full $VV/VH/\ell\nu/\ell\ell$ combination in both the $\{g_H, g_f\}$ plane, as shown in Figure 11(a), and the $\{g_q, g_\ell\}$ plane, as shown in Figure 11(b). The resulting constraints are very stringent, improving on the limits from current precision EW measurements in almost all areas of the respective planes, except at low $|g_q|$ values when considering non-universal quark and lepton couplings in the $\{g_q, g_\ell\}$ plane. This is due to the asymmetry of the precision EW measurement limits, which is related to interference effects. The constraints for HVT model A are generally stronger than for model B, due to the small fermion couplings in the latter scenario.

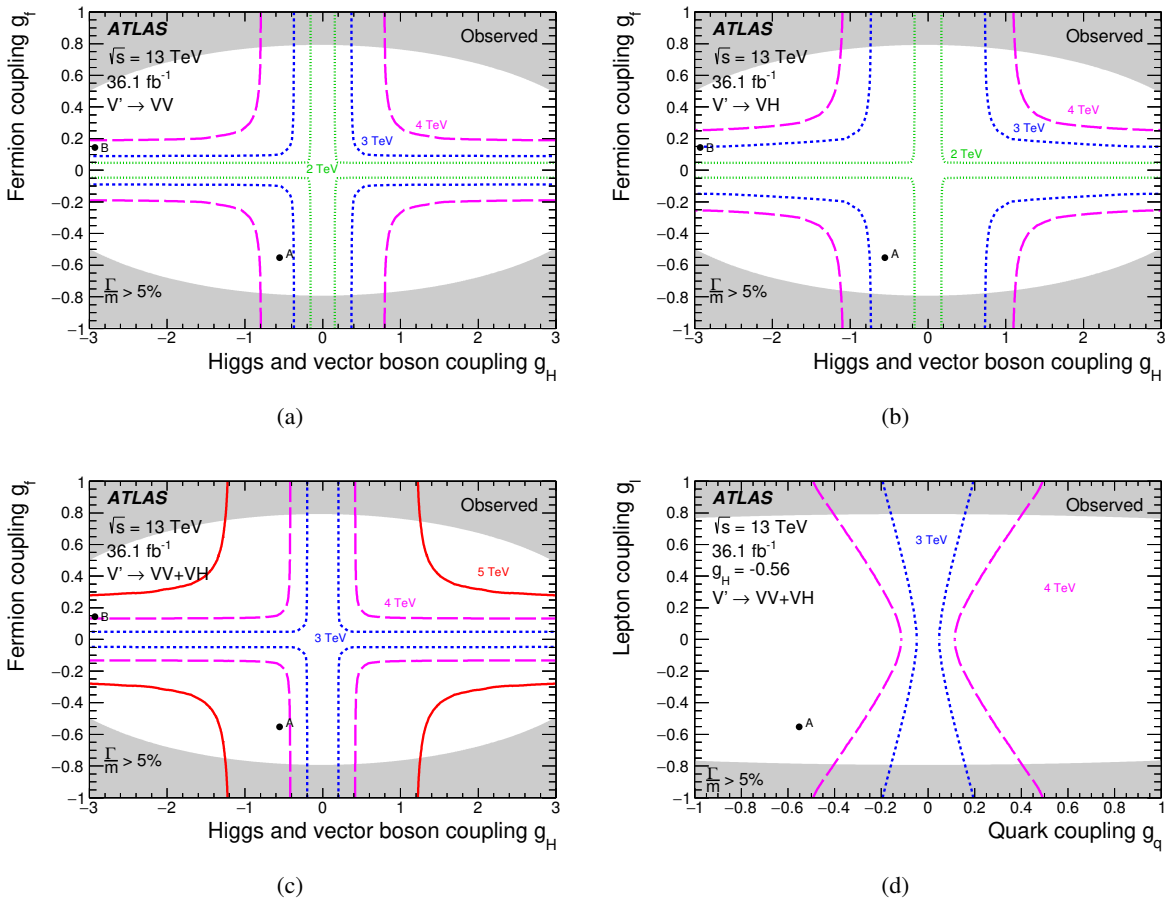

Figure 9: Observed 95% CL exclusion contours in the $\{g_H, g_f\}$ HVT parameter space for resonances of mass 2, 3, 4, or 5 TeV for (a) the VV channels, (b) the VH channels, and (c) the combined VV and VH channels; (d) shows the combined VV and VH channels in the $\{g_q, g_\ell\}$ plane with g_H set to the value from HVT model A. For (d) the 5 TeV limit contour is outside of the plane. The areas outside the curves are excluded. The gray area indicates parameter regions for which $\Gamma/m > 5\%$. Also shown are the parameters for models A and B, where applicable.

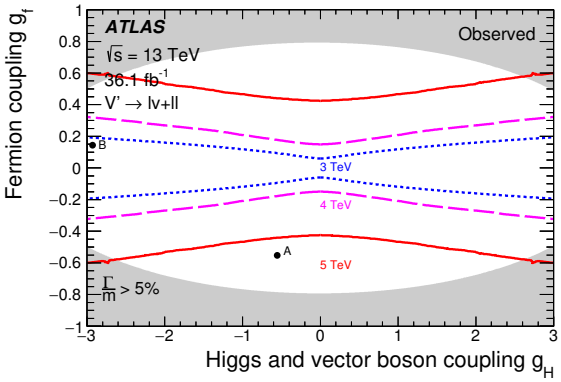

(a)

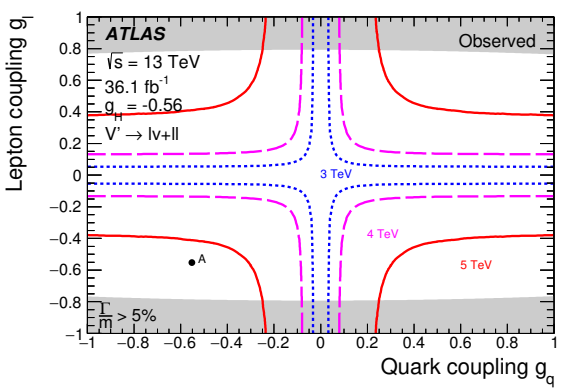

(b)

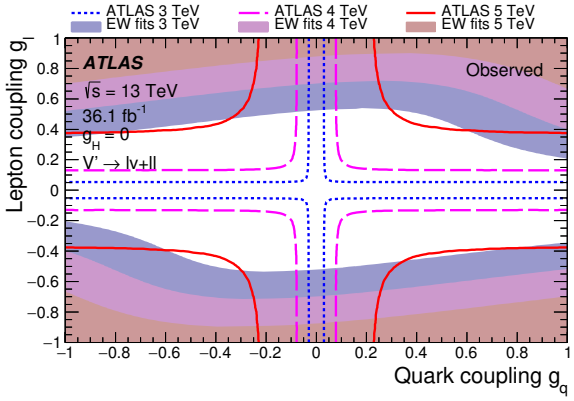

(c)

Figure 10: Observed 95% CL exclusion contours in the HVT parameter space (a) $\{g_H, g_f\}$, (b) $\{g_q, g_\ell\}$ with g_H set to the value from HVT model A, and (c) $\{g_q, g_\ell\}$ with g_H set to 0, for resonances of mass 3, 4, and 5 TeV for the $\ell\nu/\ell\ell$ channels. The areas outside the curves are excluded, as are the filled regions which show the constraints from precision EW measurements. The gray area indicates parameter regions for which $\Gamma/m > 5\%$. Also shown are the parameters for models A and B, where applicable.

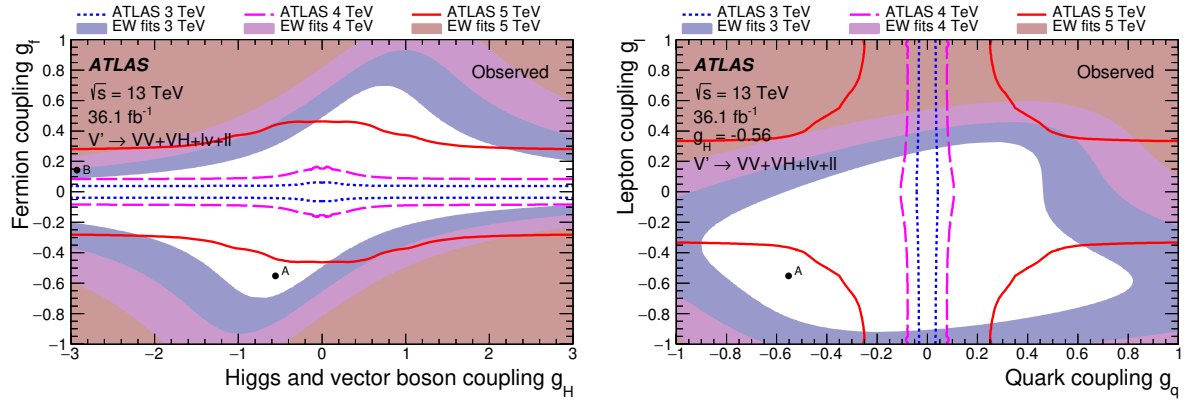

(a) (b)

Figure 11: Observed 95% CL exclusion contours in the HVT parameter space (a) $\{g_H, g_f\}$ and (b) $\{g_q, g_\ell\}$ for resonances of mass 3, 4, and 5 TeV for the combination of VV, VH, and $\ell\nu/\ell\ell$ channels. The areas outside the curves are excluded, as are the filled regions which show the constraints from precision EW measurements. Also shown are the parameters for models A and B, where applicable.

10 Conclusions

A combination of results from searches for heavy resonance production in various bosonic and leptonic final states is presented. The data were collected with the ATLAS detector at the LHC in pp collisions at $\sqrt{s} = 13$ TeV and correspond to an integrated luminosity of 36.1 fb^{-1}. While previous combination efforts included only the decays of heavy resonances into VV and VH, the combination presented here also includes decays into lepton–antilepton final states. Compared to the individual analyses, the combined results strengthen the constraints on physics beyond the Standard Model and allow the constraints to be expressed in terms of the couplings to quarks, leptons, or bosons. The relative sensitivities of the different approaches are compared, including bosonic and leptonic final states or different production mechanisms such as quark–antiquark annihilation/gluon–gluon fusion vs. vector-boson fusion.

The combined results are interpreted in the context of models with a heavy vector-boson triplet, a Kaluza–Klein excitation of the graviton or a heavy scalar singlet. The 95% CL lower limit on the mass of V' resonances in the weakly coupled HVT model A is 5.5 TeV and the corresponding limit in the strongly coupled HVT model B is 4.5 TeV. Similarly, the lower limit on the G_{KK} mass in the bulk RS model with $k/\overline{M}_{\mathrm{Pl}} = 1$ is 2.3 TeV. Limits on the cross section times branching fraction for an empirical heavy scalar model range between 380 and 1.3 fb for scalar mass values between 0.3 and 3.0 TeV in the case of production via gluon–gluon fusion. The corresponding values for scalar production via vector-boson fusion range between 140 and 3.2 fb for scalar masses between 0.5 and 3.0 TeV. Finally, the combined results are used to place stringent constraints on couplings of heavy vector bosons to quarks, leptons, and bosons. Except at low values of quark couplings where resonance production via quark–antiquark annihilation is suppressed at the LHC, these constraints are found to be more stringent than those extracted from precision electroweak measurements.

Acknowledgments

We thank CERN for the very successful operation of the LHC, as well as the support staff from our institutions without whom ATLAS could not be operated efficiently.

We acknowledge the support of ANPCyT, Argentina; YerPhI, Armenia; ARC, Australia; BMWFW and FWF, Austria; ANAS, Azerbaijan; SSTC, Belarus; CNPq and FAPESP, Brazil; NSERC, NRC and CFI, Canada; CERN; CONICYT, Chile; CAS, MOST and NSFC, China; COLCIENCIAS, Colombia; MSMT CR, MPO CR and VSC CR, Czech Republic; DNRF and DNSRC, Denmark; IN2P3-CNRS, CEA-DRF/IRFU, France; SRNSFG, Georgia; BMBF, HGF, and MPG, Germany; GSRT, Greece; RGC, Hong Kong SAR, China; ISF, I-CORE and Benoziyo Center, Israel; INFN, Italy; MEXT and JSPS, Japan; CNRST, Morocco; NWO, Netherlands; RCN, Norway; MNiSW and NCN, Poland; FCT, Portugal; MNE/IFA, Romania; MES of Russia and NRC KI, Russian Federation; JINR; MESTD, Serbia; MSSR, Slovakia; ARRS and MIZŠ, Slovenia; DST/NRF, South Africa; MINECO, Spain; SRC and Wallenberg Foundation, Sweden; SERI, SNSF and Cantons of Bern and Geneva, Switzerland; MOST, Taiwan; TAEK, Turkey; STFC, United Kingdom; DOE and NSF, United States of America. In addition, individual groups and members have received support from BCKDF, the Canada Council, CANARIE, CRC, Compute Canada, FQRNT, and the Ontario Innovation Trust, Canada; EPLANET, ERC, ERDF, FP7, Horizon 2020 and Marie Skłodowska-Curie Actions, European Union; Investissements d'Avenir Labex and Idex, ANR, Région Auvergne and Fondation Partager le Savoir, France; DFG and AvH Foundation, Germany; Herakleitos, Thales and Aristeia programmes co-financed by EU-ESF and the Greek NSRF; BSF, GIF and

Minerva, Israel; BRF, Norway; CERCA Programme Generalitat de Catalunya, Generalitat Valenciana, Spain; the Royal Society and Leverhulme Trust, United Kingdom.

The crucial computing support from all WLCG partners is acknowledged gratefully, in particular from CERN, the ATLAS Tier-1 facilities at TRIUMF (Canada), NDGF (Denmark, Norway, Sweden), CC-IN2P3 (France), KIT/GridKA (Germany), INFN-CNAF (Italy), NL-T1 (Netherlands), PIC (Spain), ASGC (Taiwan), RAL (UK) and BNL (USA), the Tier-2 facilities worldwide and large non-WLCG resource providers. Major contributors of computing resources are listed in Ref. [67].

References

[1] L. Randall and R. Sundrum, *Large Mass Hierarchy from a Small Extra Dimension*, Phys. Rev. Lett. **83** (1999) 3370, arXiv: hep-ph/9905221.

[2] G. C. Branco et al., *Theory and phenomenology of two-Higgs-doublet models*, Phys. Rept. **516** (2012) 1, arXiv: 1106.0034 [hep-ph].

[3] R. Contino, D. Marzocca, D. Pappadopulo, and R. Rattazzi, *On the effect of resonances in composite Higgs phenomenology*, JHEP **10** (2011) 081, arXiv: 1109.1570 [hep-ph].

[4] J. C. Pati and A. Salam, *Lepton number as the fourth color*, Phys. Rev. D **10** (1974) 275, Erratum: Phys. Rev. D **11** (1975) 703.

[5] H. Georgi and S. Glashow, *Unity of All Elementary-Particle Forces*, Phys. Rev. Lett. **32** (1974) 438.

[6] H. Fritzsch and P. Minkowski, *Unified interactions of leptons and hadrons*, Annals Phys. **93** (1975) 193.

[7] ATLAS Collaboration, *Searches for heavy diboson resonances in pp collisions at $\sqrt{s}$ = 13 TeV with the ATLAS detector*, JHEP **09** (2016) 173, arXiv: 1606.04833 [hep-ex].

[8] CMS Collaboration, *Combination of searches for heavy resonances decaying to WW, WZ, ZZ, WH, and ZH boson pairs in proton–proton collisions at $\sqrt{s}$ = 8 TeV and 13 TeV*, Phys. Lett. B **774** (2017) 533, arXiv: 1705.09171 [hep-ex].

[9] ATLAS Collaboration, *Search for diboson resonances with boson-tagged jets in pp collisions at $\sqrt{s}$ = 13 TeV with the ATLAS detector*, Phys. Lett. B **777** (2018) 91, arXiv: 1708.04445 [hep-ex].

[10] ATLAS Collaboration, *Search for WW/WZ resonance production in $\ell\nu qq$ final states in pp collisions at $\sqrt{s}$ = 13 TeV with the ATLAS detector*, JHEP **03** (2018) 042, arXiv: 1710.07235 [hep-ex].

[11] ATLAS Collaboration, *Search for resonant WZ production in the fully leptonic final state in proton–proton collisions at $\sqrt{s}$ = 13 TeV with the ATLAS detector*, (2018), arXiv: 1806.01532 [hep-ex].

[12] ATLAS Collaboration, *Search for heavy resonances decaying into WW in the $e\nu\mu\nu$ final state in pp collisions at $\sqrt{s}$ = 13 TeV with the ATLAS detector*, Eur. Phys. J. C **78** (2018) 24, arXiv: 1710.01123 [hep-ex].

[13] ATLAS Collaboration, *Searches for heavy ZZ and ZW resonances in the $\ell\ell qq$ and $\nu\nu qq$ final states in pp collisions at $\sqrt{s}$ = 13 TeV with the ATLAS detector*, JHEP **03** (2018) 009, arXiv: 1708.09638 [hep-ex].

[14] ATLAS Collaboration, *Search for heavy ZZ resonances in the $\ell^+\ell^-\ell^+\ell^-$ and $\ell^+\ell^-\nu\bar{\nu}$ final states using proton–proton collisions at $\sqrt{s}$ = 13 TeV with the ATLAS detector*, Eur. Phys. J. C **78** (2018) 293, arXiv: 1712.06386 [hep-ex].

[15] ATLAS Collaboration, *Search for heavy resonances decaying to a W or Z boson and a Higgs boson in the $q\bar{q}^{(\prime)}b\bar{b}$ final state in pp collisions at $\sqrt{s}$ = 13 TeV with the ATLAS detector*, Phys. Lett. B **774** (2017) 494, arXiv: 1707.06958 [hep-ex].

[16] ATLAS Collaboration, *Search for heavy resonances decaying into a W or Z boson and a Higgs boson in final states with leptons and b-jets in 36 fb^{-1} of $\sqrt{s}$ = 13 TeV pp collisions with the ATLAS detector*, JHEP **03** (2018) 174, arXiv: 1712.06518 [hep-ex].

[17] ATLAS Collaboration, *Search for a new heavy gauge boson resonance decaying into a lepton and missing transverse momentum in 36 fb^{-1} of pp collisions at $\sqrt{s}$ = 13 TeV with the ATLAS experiment*, Eur. Phys. J. C **78** (2018) 401, arXiv: 1706.04786 [hep-ex].

[18] ATLAS Collaboration, *Search for new high-mass phenomena in the dilepton final state using 36 fb^{-1} of proton–proton collision data at $\sqrt{s}$ = 13 TeV with the ATLAS detector*, JHEP **10** (2017) 182, arXiv: 1707.02424 [hep-ex].

[19] J. de Blas, J. M. Lizana, and M. Perez-Victoria, *Combining searches of Z' and W' bosons*, JHEP **01** (2013) 166, arXiv: 1211.2229 [hep-ph].

[20] D. Pappadopulo, A. Thamm, R. Torre, and A. Wulzer, *Heavy vector triplets: bridging theory and data*, JHEP **09** (2014) 060, arXiv: 1402.4431 [hep-ph].

[21] J. M. Cornwall, D. N. Levin, and G. Tiktopoulos, *Derivation of gauge invariance from high-energy unitarity bounds on the S matrix*, Phys. Rev. D **10** (1974) 1145, Erratum: Phys. Rev. D **11** (1975) 972.

[22] G. J. Gounaris, R. Kogerler, and H. Neufeld, *Relationship between longitudinally polarized vector bosons and their unphysical scalar partners*, Phys. Rev. D **34** (1986) 3257.

[23] M. S. Chanowitz and M. K. Gaillard, *The TeV physics of strongly interacting W's and Z's*, Nucl. Phys. B **261** (1985) 379.

[24] V. D. Barger, W.-Y. Keung, and E. Ma, *Gauge model with light W and Z bosons*, Phys. Rev. D **22** (1980) 727.

[25] K. Agashe, H. Davoudiasl, G. Perez, and A. Soni, *Warped gravitons at the LHC and beyond*, Phys. Rev. D **76** (2007) 036006, arXiv: hep-ph/0701186.

[26] ATLAS Collaboration, *The ATLAS Experiment at the CERN Large Hadron Collider*, JINST **3** (2008) S08003.

[27] ATLAS Collaboration, *ATLAS Insertable B-Layer Technical Design Report*, ATLAS-TDR-19, 2010, URL: https://cds.cern.ch/record/1291633, *ATLAS Insertable B-Layer Technical Design Report Addendum*, ATLAS-TDR-19-ADD-1, 2012, URL: https://cds.cern.ch/record/1451888.

[28] ATLAS Collaboration, *Performance of the ATLAS trigger system in 2015*, Eur. Phys. J. C **77** (2017) 317, arXiv: 1611.09661 [hep-ex].

[29] J. Alwall et al., *The automated computation of tree-level and next-to-leading order differential cross sections, and their matching to parton shower simulations*, JHEP **07** (2014) 079, arXiv: 1405.0301 [hep-ph].

[30] R. D. Ball et al., *Parton distributions with LHC data*, Nucl. Phys. B **867** (2013) 244, arXiv: 1207.1303 [hep-ph].

[31] S. Alioli, P. Nason, C. Oleari, and E. Re, *NLO Higgs boson production via gluon fusion matched with shower in POWHEG*, JHEP **04** (2009) 002, arXiv: 0812.0578 [hep-ph].

[32] S. Alioli, P. Nason, C. Oleari, and E. Re, *A general framework for implementing NLO calculations in shower Monte Carlo programs: the POWHEG BOX*, JHEP **06** (2010) 043, arXiv: 1002.2581 [hep-ph].

[33] H.-L. Lai et al., *New parton distributions for collider physics*, Phys. Rev. D **82** (2010) 074024, arXiv: 1007.2241 [hep-ph].

[34] T. Sjöstrand, S. Mrenna, and P. Z. Skands, *A brief introduction to PYTHIA 8.1*, Comput. Phys. Commun. **178** (2008) 852, arXiv: 0710.3820 [hep-ph].

[35] ATLAS Collaboration, *ATLAS Pythia 8 tunes to 7 TeV data*, ATL-PHYS-PUB-2014-021, 2014, URL: https://cds.cern.ch/record/1966419.

[36] ATLAS Collaboration, *Measurement of the Z/γ^* boson transverse momentum distribution in pp collisions at $\sqrt{s}$ = 7 TeV with the ATLAS detector*, JHEP **09** (2014) 145, arXiv: 1406.3660 [hep-ex].

[37] T. Gleisberg et al., *Event generation with SHERPA 1.1*, JHEP **02** (2009) 007, arXiv: 0811.4622 [hep-ph].

[38] F. Cascioli, P. Maierhofer, and S. Pozzorini, *Scattering Amplitudes with Open Loops*, Phys. Rev. Lett. **108** (2012) 111601, arXiv: 1111.5206 [hep-ph].

[39] T. Gleisberg and S. Höche, *Comix, a new matrix element generator*, JHEP **12** (2008) 039, arXiv: 0808.3674 [hep-ph].

[40] D. J. Lange, *The EvtGen particle decay simulation package*, Nucl. Instrum. Meth. A **462** (2001) 152.

[41] S. Agostinelli et al., *GEANT4 – a simulation toolkit*, Nucl. Instrum. Meth. A **506** (2003) 250.

[42] ATLAS Collaboration, *The ATLAS Simulation Infrastructure*, Eur. Phys. J. C **70** (2010) 823, arXiv: 1005.4568 [physics.ins-det].

[43] ATLAS Collaboration, *The simulation principle and performance of the ATLAS fast calorimeter simulation FastCaloSim*, ATL-PHYS-PUB-2010-013, 2010, URL: https://cds.cern.ch/record/1300517.

[44] ATLAS Collaboration, *Electron efficiency measurements with the ATLAS detector using the 2015 LHC proton–proton collision data*, ATLAS-CONF-2016-024, 2016, URL: https://cds.cern.ch/record/2157687.

[45] ATLAS Collaboration, *Muon reconstruction performance of the ATLAS detector in proton–proton collision data at $\sqrt{s}$ = 13 TeV*, Eur. Phys. J. C **76** (2016) 292, arXiv: 1603.05598 [hep-ex].

[46] ATLAS Collaboration,
Topological cell clustering in the ATLAS calorimeters and its performance in LHC Run 1,
Eur. Phys. J. C **77** (2017) 490, arXiv: 1603.02934 [hep-ex].

[47] M. Cacciari, G. P. Salam, and G. Soyez, *The anti-k_t jet clustering algorithm*, JHEP **04** (2008) 063,
arXiv: 0802.1189 [hep-ph].

[48] M. Cacciari, G. P. Salam, and G. Soyez, *FastJet user manual*, Eur. Phys. J. C **72** (2012) 1896,
arXiv: 1111.6097 [hep-ph].

[49] ATLAS Collaboration, *Performance of pile-up mitigation techniques for jets in pp collisions at $\sqrt{s}$ = 8 TeV using the ATLAS detector*, Eur. Phys. J. C **76** (2016) 581,
arXiv: 1510.03823 [hep-ex].

[50] ATLAS Collaboration, *Jet energy scale measurements and their systematic uncertainties in proton–proton collisions at $\sqrt{s}$ = 13 TeV with the ATLAS detector*,
Phys. Rev. D **96** (2017) 072002, arXiv: 1703.09665 [hep-ex].

[51] ATLAS Collaboration,
Jet energy measurement with the ATLAS detector in proton–proton collisions at $\sqrt{s}$ = 7 TeV,
Eur. Phys. J. C **73** (2013) 2304, arXiv: 1112.6426 [hep-ex].

[52] S. D. Ellis and D. E. Soper, *Successive combination jet algorithm for hadron collisions*,
Phys. Rev. D **48** (1993) 3160, arXiv: hep-ph/9305266.

[53] ATLAS Collaboration, *Identification of Boosted, Hadronically-Decaying W and Z Bosons in $\sqrt{s}$ = 13 TeV Monte Carlo Simulations for ATLAS*, ATL-PHYS-PUB-2015-033, 2015,
URL: https://cds.cern.ch/record/2041461.

[54] ATLAS Collaboration, *Performance of b-jet identification in the ATLAS experiment*,
JINST **11** (2016) P04008, arXiv: 1512.01094 [hep-ex].

[55] ATLAS Collaboration, *Optimisation of the ATLAS b-tagging performance for the 2016 LHC Run*,
ATL-PHYS-PUB-2016-012, 2016, URL: https://cds.cern.ch/record/2160731.

[56] ATLAS Collaboration, *Identification of boosted, hadronically decaying W bosons and comparisons with ATLAS data taken at $\sqrt{s}$ = 8 TeV*, Eur. Phys. J. C **76** (2016) 154,
arXiv: 1510.05821 [hep-ex].

[57] A. J. Larkoski, I. Moult, and D. Neill, *Power counting to better jet observables*,
JHEP **12** (2014) 009, arXiv: 1409.6298 [hep-ph].

[58] ATLAS Collaboration, *Performance of algorithms that reconstruct missing transverse momentum in $\sqrt{s}$ = 8 TeV proton–proton collisions in the ATLAS detector*, Eur. Phys. J. C **77** (2017) 241,
arXiv: 1609.09324 [hep-ex].

[59] S. Dulat et al.,
New parton distribution functions from a global analysis of quantum chromodynamics,
Phys. Rev. D **93** (2016) 033006, arXiv: 1506.07443 [hep-ph].

[60] ATLAS Collaboration,
Luminosity determination in pp collisions at $\sqrt{s}$ = 8 TeV using the ATLAS detector at the LHC,
Eur. Phys. J. C **76** (2016) 653, arXiv: 1608.03953 [hep-ex].

[61] W. Verkerke and D. Kirkby, *The RooFit toolkit for data modeling*, 2003,
arXiv: physics/0306116 [physics.data-an].

[62] L. Moneta et al., *The RooStats Project*, 2010, arXiv: 1009.1003 [physics.data-an].

[63] K. Cranmer, G. Lewis, L. Moneta, A. Shibata, and W. Verkerke,
HistFactory: A tool for creating statistical models for use with RooFit and RooStats,
CERN-OPEN-2012-016, 2012, URL: https://cds.cern.ch/record/1456844.

[64] G. Cowan, K. Cranmer, E. Gross, and O. Vitells,
Asymptotic formulae for likelihood-based tests of new physics, Eur. Phys. J. C **71** (2011) 1554,
arXiv: 1007.1727 [physics.data-an], Erratum: Eur. Phys. J. C **73** (2013) 2501.

[65] A. L. Read, *Presentation of search results: the CL_S technique*, J. Phys. G **28** (2002) 2693.

[66] F. del Aguila, J. de Blas, and M. Perez-Victoria,
Electroweak Limits on General New Vector Bosons, JHEP **09** (2010) 033,
arXiv: 1005.3998 [hep-ph], We thank Jorge de Blas for providing the latest constraints from electroweak precision measurements.

[67] ATLAS Collaboration, *ATLAS Computing Acknowledgements*, ATL-GEN-PUB-2016-002,
URL: https://cds.cern.ch/record/2202407.

The ATLAS Collaboration

M. Aaboud[34d], G. Aad[99], B. Abbott[124], O. Abdinov[13,*], B. Abeloos[128], D.K. Abhayasinghe[91], S.H. Abidi[164], O.S. AbouZeid[39], N.L. Abraham[153], H. Abramowicz[158], H. Abreu[157], Y. Abulaiti[6], B.S. Acharya[64a,64b,o], S. Adachi[160], L. Adamczyk[81a], J. Adelman[119], M. Adersberger[112], A. Adiguzel[12c,ah], T. Adye[141], A.A. Affolder[143], Y. Afik[157], C. Agheorghiesei[27c], J.A. Aguilar-Saavedra[136f,136a], F. Ahmadov[77,af], G. Aielli[71a,71b], S. Akatsuka[83], T.P.A. Åkesson[94], E. Akilli[52], A.V. Akimov[108], G.L. Alberghi[23b,23a], J. Albert[173], P. Albicocco[49], M.J. Alconada Verzini[86], S. Alderweireldt[117], M. Aleksa[35], I.N. Aleksandrov[77], C. Alexa[27b], T. Alexopoulos[10], M. Alhroob[124], B. Ali[138], G. Alimonti[66a], J. Alison[36], S.P. Alkire[145], C. Allaire[128], B.M.M. Allbrooke[153], B.W. Allen[127], P.P. Allport[21], A. Aloisio[67a,67b], A. Alonso[39], F. Alonso[86], C. Alpigiani[145], A.A. Alshehri[55], M.I. Alstaty[99], B. Alvarez Gonzalez[35], D. Álvarez Piqueras[171], M.G. Alviggi[67a,67b], B.T. Amadio[18], Y. Amaral Coutinho[78b], L. Ambroz[131], C. Amelung[26], D. Amidei[103], S.P. Amor Dos Santos[136a,136c], S. Amoroso[44], C.S. Amrouche[52], C. Anastopoulos[146], L.S. Ancu[52], N. Andari[142], T. Andeen[11], C.F. Anders[59b], J.K. Anders[20], K.J. Anderson[36], A. Andreazza[66a,66b], V. Andrei[59a], C.R. Anelli[173], S. Angelidakis[37], I. Angelozzi[118], A. Angerami[38], A.V. Anisenkov[120b,120a], A. Annovi[69a], C. Antel[59a], M.T. Anthony[146], M. Antonelli[49], D.J.A. Antrim[168], F. Anulli[70a], M. Aoki[79], J.A. Aparisi Pozo[171], L. Aperio Bella[35], G. Arabidze[104], J.P. Araque[136a], V. Araujo Ferraz[78b], R. Araujo Pereira[78b], A.T.H. Arce[47], R.E. Ardell[91], F.A. Arduh[86], J-F. Arguin[107], S. Argyropoulos[75], A.J. Armbruster[35], L.J. Armitage[90], A Armstrong[168], O. Arnaez[164], H. Arnold[118], M. Arratia[31], O. Arslan[24], A. Artamonov[109,*], G. Artoni[131], S. Artz[97], S. Asai[160], N. Asbah[57], E.M. Asimakopoulou[169], L. Asquith[153], K. Assamagan[29], R. Astalos[28a], R.J. Atkin[32a], M. Atkinson[170], N.B. Atlay[148], K. Augsten[138], G. Avolio[35], R. Avramidou[58a], M.K. Ayoub[15a], G. Azuelos[107,as], A.E. Baas[59a], M.J. Baca[21], H. Bachacou[142], K. Bachas[65a,65b], M. Backes[131], P. Bagnaia[70a,70b], M. Bahmani[82], H. Bahrasemani[149], A.J. Bailey[171], J.T. Baines[141], M. Bajic[39], C. Bakalis[10], O.K. Baker[180], P.J. Bakker[118], D. Bakshi Gupta[93], S. Balaji[154], E.M. Baldin[120b,120a], P. Balek[177], F. Balli[142], W.K. Balunas[133], J. Balz[97], E. Banas[82], A. Bandyopadhyay[24], S. Banerjee[178,k], A.A.E. Bannoura[179], L. Barak[158], W.M. Barbe[37], E.L. Barberio[102], D. Barberis[53b,53a], M. Barbero[99], T. Barillari[113], M-S. Barisits[35], J. Barkeloo[127], T. Barklow[150], R. Barnea[157], S.L. Barnes[58c], B.M. Barnett[141], R.M. Barnett[18], Z. Barnovska-Blenessy[58a], A. Baroncelli[72a], G. Barone[26], A.J. Barr[131], L. Barranco Navarro[171], F. Barreiro[96], J. Barreiro Guimarães da Costa[15a], R. Bartoldus[150], A.E. Barton[87], P. Bartos[28a], A. Basalaev[134], A. Bassalat[128], R.L. Bates[55], S.J. Batista[164], S. Batlamous[34e], J.R. Batley[31], M. Battaglia[143], M. Bauce[70a,70b], F. Bauer[142], K.T. Bauer[168], H.S. Bawa[150,m], J.B. Beacham[122], T. Beau[132], P.H. Beauchemin[167], P. Bechtle[24], H.C. Beck[51], H.P. Beck[20,r], K. Becker[50], M. Becker[97], C. Becot[44], A. Beddall[12d], A.J. Beddall[12a], V.A. Bednyakov[77], M. Bedognetti[118], C.P. Bee[152], T.A. Beermann[35], M. Begalli[78b], M. Begel[29], A. Behera[152], J.K. Behr[44], A.S. Bell[92], G. Bella[158], L. Bellagamba[23b], A. Bellerive[33], M. Bellomo[157], P. Bellos[9], K. Belotskiy[110], N.L. Belyaev[110], O. Benary[158,*], D. Benchekroun[34a], M. Bender[112], N. Benekos[10], Y. Benhammou[158], E. Benhar Noccioli[180], J. Benitez[75], D.P. Benjamin[47], M. Benoit[52], J.R. Bensinger[26], S. Bentvelsen[118], L. Beresford[131], M. Beretta[49], D. Berge[44], E. Bergeaas Kuutmann[169], N. Berger[5], L.J. Bergsten[26], J. Beringer[18], S. Berlendis[7], N.R. Bernard[100], G. Bernardi[132], C. Bernius[150], F.U. Bernlochner[24], T. Berry[91], P. Berta[97], C. Bertella[15a], G. Bertoli[43a,43b], I.A. Bertram[87], G.J. Besjes[39], O. Bessidskaia Bylund[179], M. Bessner[44], N. Besson[142], A. Bethani[98], S. Bethke[113], A. Betti[24], A.J. Bevan[90], J. Beyer[113], R.M. Bianchi[135], O. Biebel[112], D. Biedermann[19], R. Bielski[35], K. Bierwagen[97], N.V. Biesuz[69a,69b], M. Biglietti[72a], T.R.V. Billoud[107], M. Bindi[51], A. Bingul[12d], C. Bini[70a,70b], S. Biondi[23b,23a], M. Birman[177], T. Bisanz[51], J.P. Biswal[158], C. Bittrich[46], D.M. Bjergaard[47],

J.E. Black[150], K.M. Black[25], T. Blazek[28a], I. Bloch[44], C. Blocker[26], A. Blue[55], U. Blumenschein[90], Dr. Blunier[144a], G.J. Bobbink[118], V.S. Bobrovnikov[120b,120a], S.S. Bocchetta[94], A. Bocci[47], D. Boerner[179], D. Bogavac[112], A.G. Bogdanchikov[120b,120a], C. Bohm[43a], V. Boisvert[91], P. Bokan[169,51], T. Bold[81a], A.S. Boldyrev[111], A.E. Bolz[59b], M. Bomben[132], M. Bona[90], J.S. Bonilla[127], M. Boonekamp[142], A. Borisov[140], G. Borissov[87], J. Bortfeldt[35], D. Bortoletto[131], V. Bortolotto[71a,71b], D. Boscherini[23b], M. Bosman[14], J.D. Bossio Sola[30], K. Bouaouda[34a], J. Boudreau[135], E.V. Bouhova-Thacker[87], D. Boumediene[37], C. Bourdarios[128], S.K. Boutle[55], A. Boveia[122], J. Boyd[35], D. Boye[32b], I.R. Boyko[77], A.J. Bozson[91], J. Bracinik[21], N. Brahimi[99], A. Brandt[8], G. Brandt[179], O. Brandt[59a], F. Braren[44], U. Bratzler[161], B. Brau[100], J.E. Brau[127], W.D. Breaden Madden[55], K. Brendlinger[44], L. Brenner[44], R. Brenner[169], S. Bressler[177], B. Brickwedde[97], D.L. Briglin[21], D. Britton[55], D. Britzger[59b], I. Brock[24], R. Brock[104], G. Brooijmans[38], T. Brooks[91], W.K. Brooks[144b], E. Brost[119], J.H Broughton[21], P.A. Bruckman de Renstrom[82], D. Bruncko[28b], A. Bruni[23b], G. Bruni[23b], L.S. Bruni[118], S. Bruno[71a,71b], B.H. Brunt[31], M. Bruschi[23b], N. Bruscino[135], P. Bryant[36], L. Bryngemark[44], T. Buanes[17], Q. Buat[35], P. Buchholz[148], A.G. Buckley[55], I.A. Budagov[77], F. Buehrer[50], M.K. Bugge[130], O. Bulekov[110], D. Bullock[8], T.J. Burch[119], S. Burdin[88], C.D. Burgard[118], A.M. Burger[5], B. Burghgrave[119], K. Burka[82], S. Burke[141], I. Burmeister[45], J.T.P. Burr[131], V. Büscher[97], E. Buschmann[51], P. Bussey[55], J.M. Butler[25], C.M. Buttar[55], J.M. Butterworth[92], P. Butti[35], W. Buttinger[35], A. Buzatu[155], A.R. Buzykaev[120b,120a], G. Cabras[23b,23a], S. Cabrera Urbán[171], D. Caforio[138], H. Cai[170], V.M.M. Cairo[2], O. Cakir[4a], N. Calace[52], P. Calafiura[18], A. Calandri[99], G. Calderini[132], P. Calfayan[63], G. Callea[40b,40a], L.P. Caloba[78b], S. Calvente Lopez[96], D. Calvet[37], S. Calvet[37], T.P. Calvet[152], M. Calvetti[69a,69b], R. Camacho Toro[132], S. Camarda[35], P. Camarri[71a,71b], D. Cameron[130], R. Caminal Armadans[100], C. Camincher[35], S. Campana[35], M. Campanelli[92], A. Camplani[39], A. Campoverde[148], V. Canale[67a,67b], M. Cano Bret[58c], J. Cantero[125], T. Cao[158], Y. Cao[170], M.D.M. Capeans Garrido[35], I. Caprini[27b], M. Caprini[27b], M. Capua[40b,40a], R.M. Carbone[38], R. Cardarelli[71a], F.C. Cardillo[146], I. Carli[139], T. Carli[35], G. Carlino[67a], B.T. Carlson[135], L. Carminati[66a,66b], R.M.D. Carney[43a,43b], S. Caron[117], E. Carquin[144b], S. Carrá[66a,66b], G.D. Carrillo-Montoya[35], D. Casadei[32b], M.P. Casado[14,f], A.F. Casha[164], D.W. Casper[168], R. Castelijn[118], F.L. Castillo[171], V. Castillo Gimenez[171], N.F. Castro[136a,136e], A. Catinaccio[35], J.R. Catmore[130], A. Cattai[35], J. Caudron[24], V. Cavaliere[29], E. Cavallaro[14], D. Cavalli[66a], M. Cavalli-Sforza[14], V. Cavasinni[69a,69b], E. Celebi[12b], F. Ceradini[72a,72b], L. Cerda Alberich[171], A.S. Cerqueira[78a], A. Cerri[153], L. Cerrito[71a,71b], F. Cerutti[18], A. Cervelli[23b,23a], S.A. Cetin[12b], A. Chafaq[34a], D Chakraborty[119], S.K. Chan[57], W.S. Chan[118], Y.L. Chan[61a], J.D. Chapman[31], B. Chargeishvili[156b], D.G. Charlton[21], C.C. Chau[33], C.A. Chavez Barajas[153], S. Che[122], A. Chegwidden[104], S. Chekanov[6], S.V. Chekulaev[165a], G.A. Chelkov[77,ar], M.A. Chelstowska[35], C. Chen[58a], C.H. Chen[76], H. Chen[29], J. Chen[58a], J. Chen[38], S. Chen[133], S.J. Chen[15c], X. Chen[15b,aq], Y. Chen[80], Y-H. Chen[44], H.C. Cheng[103], H.J. Cheng[15d], A. Cheplakov[77], E. Cheremushkina[140], R. Cherkaoui El Moursli[34e], E. Cheu[7], K. Cheung[62], L. Chevalier[142], V. Chiarella[49], G. Chiarelli[69a], G. Chiodini[65a], A.S. Chisholm[35,21], A. Chitan[27b], I. Chiu[160], Y.H. Chiu[173], M.V. Chizhov[77], K. Choi[63], A.R. Chomont[128], S. Chouridou[159], Y.S. Chow[118], V. Christodoulou[92], M.C. Chu[61a], J. Chudoba[137], A.J. Chuinard[101], J.J. Chwastowski[82], L. Chytka[126], D. Cinca[45], V. Cindro[89], I.A. Cioară[24], A. Ciocio[18], F. Cirotto[67a,67b], Z.H. Citron[177], M. Citterio[66a], A. Clark[52], M.R. Clark[38], P.J. Clark[48], C. Clement[43a,43b], Y. Coadou[99], M. Cobal[64a,64c], A. Coccaro[53b,53a], J. Cochran[76], H. Cohen[158], A.E.C. Coimbra[177], L. Colasurdo[117], B. Cole[38], A.P. Colijn[118], J. Collot[56], P. Conde Muiño[136a,136b], E. Coniavitis[50], S.H. Connell[32b], I.A. Connelly[98], S. Constantinescu[27b], F. Conventi[67a,at], A.M. Cooper-Sarkar[131], F. Cormier[172], K.J.R. Cormier[164], L.D. Corpe[92], M. Corradi[70a,70b], E.E. Corrigan[94], F. Corriveau[101,ad], A. Cortes-Gonzalez[35], M.J. Costa[171], F. Costanza[5], D. Costanzo[146], G. Cottin[31], G. Cowan[91], B.E. Cox[98], J. Crane[98], K. Cranmer[121], S.J. Crawley[55], R.A. Creager[133], G. Cree[33], S. Crépé-Renaudin[56], F. Crescioli[132], M. Cristinziani[24], V. Croft[121], G. Crosetti[40b,40a], A. Cueto[96], T. Cuhadar Donszelmann[146],

A.R. Cukierman[150], S. Czekierda[82], P. Czodrowski[35], M.J. Da Cunha Sargedas De Sousa[58b,136b], C. Da Via[98], W. Dabrowski[81a], T. Dado[28a,y], S. Dahbi[34e], T. Dai[103], F. Dallaire[107], C. Dallapiccola[100], M. Dam[39], G. D'amen[23b,23a], J. Damp[97], J.R. Dandoy[133], M.F. Daneri[30], N.P. Dang[178,k], N.D Dann[98], M. Danninger[172], V. Dao[35], G. Darbo[53b], S. Darmora[8], O. Dartsi[5], A. Dattagupta[127], T. Daubney[44], S. D'Auria[55], W. Davey[24], C. David[44], T. Davidek[139], D.R. Davis[47], E. Dawe[102], I. Dawson[146], K. De[8], R. De Asmundis[67a], A. De Benedetti[124], M. De Beurs[118], S. De Castro[23b,23a], S. De Cecco[70a,70b], N. De Groot[117], P. de Jong[118], H. De la Torre[104], F. De Lorenzi[76], A. De Maria[51,t], D. De Pedis[70a], A. De Salvo[70a], U. De Sanctis[71a,71b], M. De Santis[71a,71b], A. De Santo[153], K. De Vasconcelos Corga[99], J.B. De Vivie De Regie[128], C. Debenedetti[143], D.V. Dedovich[77], N. Dehghanian[3], M. Del Gaudio[40b,40a], J. Del Peso[96], Y. Delabat Diaz[44], D. Delgove[128], F. Deliot[142], C.M. Delitzsch[7], M. Della Pietra[67a,67b], D. Della Volpe[52], A. Dell'Acqua[35], L. Dell'Asta[25], M. Delmastro[5], C. Delporte[128], P.A. Delsart[56], D.A. DeMarco[164], S. Demers[180], M. Demichev[77], S.P. Denisov[140], D. Denysiuk[118], L. D'Eramo[132], D. Derendarz[82], J.E. Derkaoui[34d], F. Derue[132], P. Dervan[88], K. Desch[24], C. Deterre[44], K. Dette[164], M.R. Devesa[30], P.O. Deviveiros[35], A. Dewhurst[141], S. Dhaliwal[26], F.A. Di Bello[52], A. Di Ciaccio[71a,71b], L. Di Ciaccio[5], W.K. Di Clemente[133], C. Di Donato[67a,67b], A. Di Girolamo[35], B. Di Micco[72a,72b], R. Di Nardo[100], K.F. Di Petrillo[57], R. Di Sipio[164], D. Di Valentino[33], C. Diaconu[99], M. Diamond[164], F.A. Dias[39], T. Dias Do Vale[136a], M.A. Diaz[144a], J. Dickinson[18], E.B. Diehl[103], J. Dietrich[19], S. Díez Cornell[44], A. Dimitrievska[18], J. Dingfelder[24], F. Dittus[35], F. Djama[99], T. Djobava[156b], J.I. Djuvsland[59a], M.A.B. Do Vale[78c], M. Dobre[27b], D. Dodsworth[26], C. Doglioni[94], J. Dolejsi[139], Z. Dolezal[139], M. Donadelli[78d], J. Donini[37], A. D'onofrio[90], M. D'Onofrio[88], J. Dopke[141], A. Doria[67a], M.T. Dova[86], A.T. Doyle[55], E. Drechsler[51], E. Dreyer[149], T. Dreyer[51], Y. Du[58b], F. Dubinin[108], M. Dubovsky[28a], A. Dubreuil[52], E. Duchovni[177], G. Duckeck[112], A. Ducourthial[132], O.A. Ducu[107,x], D. Duda[113], A. Dudarev[35], A.C. Dudder[97], E.M. Duffield[18], L. Duflot[128], M. Dührssen[35], C. Dülsen[179], M. Dumancic[177], A.E. Dumitriu[27b,d], A.K. Duncan[55], M. Dunford[59a], A. Duperrin[99], H. Duran Yildiz[4a], M. Düren[54], A. Durglishvili[156b], D. Duschinger[46], B. Dutta[44], D. Duvnjak[1], M. Dyndal[44], S. Dysch[98], B.S. Dziedzic[82], C. Eckardt[44], K.M. Ecker[113], R.C. Edgar[103], T. Eifert[35], G. Eigen[17], K. Einsweiler[18], T. Ekelof[169], M. El Kacimi[34c], R. El Kosseifi[99], V. Ellajosyula[99], M. Ellert[169], F. Ellinghaus[179], A.A. Elliot[90], N. Ellis[35], J. Elmsheuser[29], M. Elsing[35], D. Emeliyanov[141], Y. Enari[160], J.S. Ennis[175], M.B. Epland[47], J. Erdmann[45], A. Ereditato[20], S. Errede[170], M. Escalier[128], C. Escobar[171], O. Estrada Pastor[171], A.I. Etienvre[142], E. Etzion[158], H. Evans[63], A. Ezhilov[134], M. Ezzi[34e], F. Fabbri[55], L. Fabbri[23b,23a], V. Fabiani[117], G. Facini[92], R.M. Faisca Rodrigues Pereira[136a], R.M. Fakhrutdinov[140], S. Falciano[70a], P.J. Falke[5], S. Falke[5], J. Faltova[139], Y. Fang[15a], M. Fanti[66a,66b], A. Farbin[8], A. Farilla[72a], E.M. Farina[68a,68b], T. Farooque[104], S. Farrell[18], S.M. Farrington[175], P. Farthouat[35], F. Fassi[34e], P. Fassnacht[35], D. Fassouliotis[9], M. Faucci Giannelli[48], A. Favareto[53b,53a], W.J. Fawcett[31], L. Fayard[128], O.L. Fedin[134,p], W. Fedorko[172], M. Feickert[41], S. Feigl[130], L. Feligioni[99], C. Feng[58b], E.J. Feng[35], M. Feng[47], M.J. Fenton[55], A.B. Fenyuk[140], L. Feremenga[8], J. Ferrando[44], A. Ferrari[169], P. Ferrari[118], R. Ferrari[68a], D.E. Ferreira de Lima[59b], A. Ferrer[171], D. Ferrere[52], C. Ferretti[103], F. Fiedler[97], A. Filipčič[89], F. Filthaut[117], K.D. Finelli[25], M.C.N. Fiolhais[136a,136c,a], L. Fiorini[171], C. Fischer[14], W.C. Fisher[104], N. Flaschel[44], I. Fleck[148], P. Fleischmann[103], R.R.M. Fletcher[133], T. Flick[179], B.M. Flierl[112], L.M. Flores[133], L.R. Flores Castillo[61a], F.M. Follega[73a,73b], N. Fomin[17], G.T. Forcolin[73a,73b], A. Formica[142], F.A. Förster[14], A.C. Forti[98], A.G. Foster[21], D. Fournier[128], H. Fox[87], S. Fracchia[146], P. Francavilla[69a,69b], M. Franchini[23b,23a], S. Franchino[59a], D. Francis[35], L. Franconi[130], M. Franklin[57], M. Frate[168], M. Fraternali[68a,68b], A.N. Fray[90], D. Freeborn[92], S.M. Fressard-Batraneanu[35], B. Freund[107], W.S. Freund[78b], E.M. Freundlich[45], D.C. Frizzell[124], D. Froidevaux[35], J.A. Frost[131], C. Fukunaga[161], E. Fullana Torregrosa[171], T. Fusayasu[114], J. Fuster[171], O. Gabizon[157], A. Gabrielli[23b,23a], A. Gabrielli[18], G.P. Gach[81a], S. Gadatsch[52], P. Gadow[113], G. Gagliardi[53b,53a], L.G. Gagnon[107], C. Galea[27b], B. Galhardo[136a,136c], E.J. Gallas[131], B.J. Gallop[141],

P. Gallus[138], G. Galster[39], R. Gamboa Goni[90], K.K. Gan[122], S. Ganguly[177], J. Gao[58a], Y. Gao[88], Y.S. Gao[150,m], C. García[171], J.E. García Navarro[171], J.A. García Pascual[15a], M. Garcia-Sciveres[18], R.W. Gardner[36], N. Garelli[150], V. Garonne[130], K. Gasnikova[44], A. Gaudiello[53b,53a], G. Gaudio[68a], I.L. Gavrilenko[108], A. Gavrilyuk[109], C. Gay[172], G. Gaycken[24], E.N. Gazis[10], C.N.P. Gee[141], J. Geisen[51], M. Geisen[97], M.P. Geisler[59a], K. Gellerstedt[43a,43b], C. Gemme[53b], M.H. Genest[56], C. Geng[103], S. Gentile[70a,70b], S. George[91], D. Gerbaudo[14], G. Gessner[45], S. Ghasemi[148], M. Ghasemi Bostanabad[173], M. Ghneimat[24], B. Giacobbe[23b], S. Giagu[70a,70b], N. Giangiacomi[23b,23a], P. Giannetti[69a], A. Giannini[67a,67b], S.M. Gibson[91], M. Gignac[143], D. Gillberg[33], G. Gilles[179], D.M. Gingrich[3,as], M.P. Giordani[64a,64c], F.M. Giorgi[23b], P.F. Giraud[142], P. Giromini[57], G. Giugliarelli[64a,64c], D. Giugni[66a], F. Giuli[131], M. Giulini[59b], S. Gkaitatzis[159], I. Gkialas[9,j], E.L. Gkougkousis[14], P. Gkountoumis[10], L.K. Gladilin[111], C. Glasman[96], J. Glatzer[14], P.C.F. Glaysher[44], A. Glazov[44], M. Goblirsch-Kolb[26], J. Godlewski[82], S. Goldfarb[102], T. Golling[52], D. Golubkov[140], A. Gomes[136a,136b,136d], R. Goncalves Gama[78a], R. Gonçalo[136a], G. Gonella[50], L. Gonella[21], A. Gongadze[77], F. Gonnella[21], J.L. Gonski[57], S. González de la Hoz[171], S. Gonzalez-Sevilla[52], L. Goossens[35], P.A. Gorbounov[109], H.A. Gordon[29], B. Gorini[35], E. Gorini[65a,65b], A. Gorišek[89], A.T. Goshaw[47], C. Gössling[45], M.I. Gostkin[77], C.A. Gottardo[24], C.R. Goudet[128], D. Goujdami[34c], A.G. Goussiou[145], N. Govender[32b,b], C. Goy[5], E. Gozani[157], I. Grabowska-Bold[81a], P.O.J. Gradin[169], E.C. Graham[88], J. Gramling[168], E. Gramstad[130], S. Grancagnolo[19], V. Gratchev[134], P.M. Gravila[27f], F.G. Gravili[65a,65b], C. Gray[55], H.M. Gray[18], Z.D. Greenwood[93,aj], C. Grefe[24], K. Gregersen[94], I.M. Gregor[44], P. Grenier[150], K. Grevtsov[44], N.A. Grieser[124], J. Griffiths[8], A.A. Grillo[143], K. Grimm[150], S. Grinstein[14,z], Ph. Gris[37], J.-F. Grivaz[128], S. Groh[97], E. Gross[177], J. Grosse-Knetter[51], G.C. Grossi[93], Z.J. Grout[92], C. Grud[103], A. Grummer[116], L. Guan[103], W. Guan[178], J. Guenther[35], A. Guerguichon[128], F. Guescini[165a], D. Guest[168], R. Gugel[50], B. Gui[122], T. Guillemin[5], S. Guindon[35], U. Gul[55], C. Gumpert[35], J. Guo[58c], W. Guo[103], Y. Guo[58a,s], Z. Guo[99], R. Gupta[41], S. Gurbuz[12c], G. Gustavino[124], B.J. Gutelman[157], P. Gutierrez[124], C. Gutschow[92], C. Guyot[142], M.P. Guzik[81a], C. Gwenlan[131], C.B. Gwilliam[88], A. Haas[121], C. Haber[18], H.K. Hadavand[8], N. Haddad[34e], A. Hadef[58a], S. Hageböck[24], M. Hagihara[166], H. Hakobyan[181,*], M. Haleem[174], J. Haley[125], G. Halladjian[104], G.D. Hallewell[99], K. Hamacher[179], P. Hamal[126], K. Hamano[173], A. Hamilton[32a], G.N. Hamity[146], K. Han[58a,ai], L. Han[58a], S. Han[15d], K. Hanagaki[79,v], M. Hance[143], D.M. Handl[112], B. Haney[133], R. Hankache[132], P. Hanke[59a], E. Hansen[94], J.B. Hansen[39], J.D. Hansen[39], M.C. Hansen[24], P.H. Hansen[39], K. Hara[166], A.S. Hard[178], T. Harenberg[179], S. Harkusha[105], P.F. Harrison[175], N.M. Hartmann[112], Y. Hasegawa[147], A. Hasib[48], S. Hassani[142], S. Haug[20], R. Hauser[104], L. Hauswald[46], L.B. Havener[38], M. Havranek[138], C.M. Hawkes[21], R.J. Hawkings[35], D. Hayden[104], C. Hayes[152], C.P. Hays[131], J.M. Hays[90], H.S. Hayward[88], S.J. Haywood[141], M.P. Heath[48], V. Hedberg[94], L. Heelan[8], S. Heer[24], K.K. Heidegger[50], J. Heilman[33], S. Heim[44], T. Heim[18], B. Heinemann[44,an], J.J. Heinrich[112], L. Heinrich[121], C. Heinz[54], J. Hejbal[137], L. Helary[35], A. Held[172], S. Hellesund[130], S. Hellman[43a,43b], C. Helsens[35], R.C.W. Henderson[87], Y. Heng[178], S. Henkelmann[172], A.M. Henriques Correia[35], G.H. Herbert[19], H. Herde[26], V. Herget[174], Y. Hernández Jiménez[32c], H. Herr[97], M.G. Herrmann[112], G. Herten[50], R. Hertenberger[112], L. Hervas[35], T.C. Herwig[133], G.G. Hesketh[92], N.P. Hessey[165a], J.W. Hetherly[41], S. Higashino[79], E. Higón-Rodriguez[171], K. Hildebrand[36], E. Hill[173], J.C. Hill[31], K.K. Hill[29], K.H. Hiller[44], S.J. Hillier[21], M. Hils[46], I. Hinchliffe[18], M. Hirose[129], D. Hirschbuehl[179], B. Hiti[89], O. Hladik[137], D.R. Hlaluku[32c], X. Hoad[48], J. Hobbs[152], N. Hod[165a], M.C. Hodgkinson[146], A. Hoecker[35], M.R. Hoeferkamp[116], F. Hoenig[112], D. Hohn[24], D. Hohov[128], T.R. Holmes[36], M. Holzbock[112], M. Homann[45], S. Honda[166], T. Honda[79], T.M. Hong[135], A. Hönle[113], B.H. Hooberman[170], W.H. Hopkins[127], Y. Horii[115], P. Horn[46], A.J. Horton[149], L.A. Horyn[36], J-Y. Hostachy[56], A. Hostiuc[145], S. Hou[155], A. Hoummada[34a], J. Howarth[98], J. Hoya[86], M. Hrabovsky[126], I. Hristova[19], J. Hrivnac[128], A. Hrynevich[106], T. Hryn'ova[5], P.J. Hsu[62], S.-C. Hsu[145], Q. Hu[29], S. Hu[58c], Y. Huang[15a], Z. Hubacek[138], F. Hubaut[99], M. Huebner[24],

F. Huegging[24], T.B. Huffman[131], E.W. Hughes[38], M. Huhtinen[35], R.F.H. Hunter[33], P. Huo[152], A.M. Hupe[33], N. Huseynov[77,af], J. Huston[104], J. Huth[57], R. Hyneman[103], G. Iacobucci[52], G. Iakovidis[29], I. Ibragimov[148], L. Iconomidou-Fayard[128], Z. Idrissi[34e], P. Iengo[35], R. Ignazzi[39], O. Igonkina[118,ab], R. Iguchi[160], T. Iizawa[52], Y. Ikegami[79], M. Ikeno[79], D. Iliadis[159], N. Ilic[150], F. Iltzsche[46], G. Introzzi[68a,68b], M. Iodice[72a], K. Iordanidou[38], V. Ippolito[70a,70b], M.F. Isacson[169], N. Ishijima[129], M. Ishino[160], M. Ishitsuka[162], W. Islam[125], C. Issever[131], S. Istin[157], F. Ito[166], J.M. Iturbe Ponce[61a], R. Iuppa[73a,73b], A. Ivina[177], H. Iwasaki[79], J.M. Izen[42], V. Izzo[67a], P. Jacka[137], P. Jackson[1], R.M. Jacobs[24], V. Jain[2], G. Jäkel[179], K.B. Jakobi[97], K. Jakobs[50], S. Jakobsen[74], T. Jakoubek[137], D.O. Jamin[125], D.K. Jana[93], R. Jansky[52], J. Janssen[24], M. Janus[51], P.A. Janus[81a], G. Jarlskog[94], N. Javadov[77,af], T. Javůrek[35], M. Javurkova[50], F. Jeanneau[142], L. Jeanty[18], J. Jejelava[156a,ag], A. Jelinskas[175], P. Jenni[50,c], J. Jeong[44], N. Jeong[44], S. Jézéquel[5], H. Ji[178], J. Jia[152], H. Jiang[76], Y. Jiang[58a], Z. Jiang[150,q], S. Jiggins[50], F.A. Jimenez Morales[37], J. Jimenez Pena[171], S. Jin[15c], A. Jinaru[27b], O. Jinnouchi[162], H. Jivan[32c], P. Johansson[146], K.A. Johns[7], C.A. Johnson[63], W.J. Johnson[145], K. Jon-And[43a,43b], R.W.L. Jones[87], S.D. Jones[153], S. Jones[7], T.J. Jones[88], J. Jongmanns[59a], P.M. Jorge[136a,136b], J. Jovicevic[165a], X. Ju[18], J.J. Junggeburth[113], A. Juste Rozas[14,z], A. Kaczmarska[82], M. Kado[128], H. Kagan[122], M. Kagan[150], T. Kaji[176], E. Kajomovitz[157], C.W. Kalderon[94], A. Kaluza[97], S. Kama[41], A. Kamenshchikov[140], L. Kanjir[89], Y. Kano[160], V.A. Kantserov[110], J. Kanzaki[79], B. Kaplan[121], L.S. Kaplan[178], D. Kar[32c], M.J. Kareem[165b], E. Karentzos[10], S.N. Karpov[77], Z.M. Karpova[77], V. Kartvelishvili[87], A.N. Karyukhin[140], L. Kashif[178], R.D. Kass[122], A. Kastanas[151], Y. Kataoka[160], C. Kato[58d,58c], J. Katzy[44], K. Kawade[80], K. Kawagoe[85], T. Kawamoto[160], G. Kawamura[51], E.F. Kay[88], V.F. Kazanin[120b,120a], R. Keeler[173], R. Kehoe[41], J.S. Keller[33], E. Kellermann[94], J.J. Kempster[21], J. Kendrick[21], O. Kepka[137], S. Kersten[179], B.P. Kerševan[89], R.A. Keyes[101], M. Khader[170], F. Khalil-Zada[13], A. Khanov[125], A.G. Kharlamov[120b,120a], T. Kharlamova[120b,120a], E.E. Khoda[172], A. Khodinov[163], T.J. Khoo[52], E. Khramov[77], J. Khubua[156b], S. Kido[80], M. Kiehn[52], C.R. Kilby[91], Y.K. Kim[36], N. Kimura[64a,64c], O.M. Kind[19], B.T. King[88], D. Kirchmeier[46], J. Kirk[141], A.E. Kiryunin[113], T. Kishimoto[160], D. Kisielewska[81a], V. Kitali[44], O. Kivernyk[5], E. Kladiva[28b], T. Klapdor-Kleingrothaus[50], M.H. Klein[103], M. Klein[88], U. Klein[88], K. Kleinknecht[97], P. Klimek[119], A. Klimentov[29], R. Klingenberg[45,*], T. Klingl[24], T. Klioutchnikova[35], F.F. Klitzner[112], P. Kluit[118], S. Kluth[113], E. Kneringer[74], E.B.F.G. Knoops[99], A. Knue[50], A. Kobayashi[160], D. Kobayashi[85], T. Kobayashi[160], M. Kobel[46], M. Kocian[150], P. Kodys[139], P.T. Koenig[24], T. Koffas[33], E. Koffeman[118], N.M. Köhler[113], T. Koi[150], M. Kolb[59b], I. Koletsou[5], T. Kondo[79], N. Kondrashova[58c], K. Köneke[50], A.C. König[117], T. Kono[79], R. Konoplich[121,ak], V. Konstantinides[92], N. Konstantinidis[92], B. Konya[94], R. Kopeliansky[63], S. Koperny[81a], K. Korcyl[82], K. Kordas[159], G. Koren[158], A. Korn[92], I. Korolkov[14], E.V. Korolkova[146], N. Korotkova[111], O. Kortner[113], S. Kortner[113], T. Kosek[139], V.V. Kostyukhin[24], A. Kotwal[47], A. Koulouris[10], A. Kourkoumeli-Charalampidi[68a,68b], C. Kourkoumelis[9], E. Kourlitis[146], V. Kouskoura[29], A.B. Kowalewska[82], R. Kowalewski[173], T.Z. Kowalski[81a], C. Kozakai[160], W. Kozanecki[142], A.S. Kozhin[140], V.A. Kramarenko[111], G. Kramberger[89], D. Krasnopevtsev[58a], M.W. Krasny[132], A. Krasznahorkay[35], D. Krauss[113], J.A. Kremer[81a], J. Kretzschmar[88], P. Krieger[164], K. Krizka[18], K. Kroeninger[45], H. Kroha[113], J. Kroll[137], J. Kroll[133], J. Krstic[16], U. Kruchonak[77], H. Krüger[24], N. Krumnack[76], M.C. Kruse[47], T. Kubota[102], S. Kuday[4b], J.T. Kuechler[179], S. Kuehn[35], A. Kugel[59a], F. Kuger[174], T. Kuhl[44], V. Kukhtin[77], R. Kukla[99], Y. Kulchitsky[105], S. Kuleshov[144b], Y.P. Kulinich[170], M. Kuna[56], T. Kunigo[83], A. Kupco[137], T. Kupfer[45], O. Kuprash[158], H. Kurashige[80], L.L. Kurchaninov[165a], Y.A. Kurochkin[105], M.G. Kurth[15d], E.S. Kuwertz[35], M. Kuze[162], J. Kvita[126], T. Kwan[101], A. La Rosa[113], J.L. La Rosa Navarro[78d], L. La Rotonda[40b,40a], F. La Ruffa[40b,40a], C. Lacasta[171], F. Lacava[70a,70b], J. Lacey[44], D.P.J. Lack[98], H. Lacker[19], D. Lacour[132], E. Ladygin[77], R. Lafaye[5], B. Laforge[132], T. Lagouri[32c], S. Lai[51], S. Lammers[63], W. Lampl[7], E. Lançon[29], U. Landgraf[50], M.P.J. Landon[90], M.C. Lanfermann[52], V.S. Lang[44], J.C. Lange[14], R.J. Langenberg[35],

A.J. Lankford[168], F. Lanni[29], K. Lantzsch[24], A. Lanza[68a], A. Lapertosa[53b,53a], S. Laplace[132], J.F. Laporte[142], T. Lari[66a], F. Lasagni Manghi[23b,23a], M. Lassnig[35], T.S. Lau[61a], A. Laudrain[128], M. Lavorgna[67a,67b], A.T. Law[143], M. Lazzaroni[66a,66b], B. Le[102], O. Le Dortz[132], E. Le Guirriec[99], E.P. Le Quilleuc[142], M. LeBlanc[7], T. LeCompte[6], F. Ledroit-Guillon[56], C.A. Lee[29], G.R. Lee[144a], L. Lee[57], S.C. Lee[155], B. Lefebvre[101], M. Lefebvre[173], F. Legger[112], C. Leggett[18], K. Lehmann[149], N. Lehmann[179], G. Lehmann Miotto[35], W.A. Leight[44], A. Leisos[159,w], M.A.L. Leite[78d], R. Leitner[139], D. Lellouch[177], B. Lemmer[51], K.J.C. Leney[92], T. Lenz[24], B. Lenzi[35], R. Leone[7], S. Leone[69a], C. Leonidopoulos[48], G. Lerner[153], C. Leroy[107], R. Les[164], A.A.J. Lesage[142], C.G. Lester[31], M. Levchenko[134], J. Levêque[5], D. Levin[103], L.J. Levinson[177], D. Lewis[90], B. Li[103], C-Q. Li[58a], H. Li[58b], L. Li[58c], M. Li[15a], Q. Li[15d], Q.Y. Li[58a], S. Li[58d,58c], X. Li[58c], Y. Li[148], Z. Liang[15a], B. Liberti[71a], A. Liblong[164], K. Lie[61c], S. Liem[118], A. Limosani[154], C.Y. Lin[31], K. Lin[104], T.H. Lin[97], R.A. Linck[63], J.H. Lindon[21], B.E. Lindquist[152], A.L. Lionti[52], E. Lipeles[133], A. Lipniacka[17], M. Lisovyi[59b], T.M. Liss[170,ap], A. Lister[172], A.M. Litke[143], J.D. Little[8], B. Liu[76], B.L Liu[6], H.B. Liu[29], H. Liu[103], J.B. Liu[58a], J.K.K. Liu[131], K. Liu[132], M. Liu[58a], P. Liu[18], Y. Liu[15a], Y.L. Liu[58a], Y.W. Liu[58a], M. Livan[68a,68b], A. Lleres[56], J. Llorente Merino[15a], S.L. Lloyd[90], C.Y. Lo[61b], F. Lo Sterzo[41], E.M. Lobodzinska[44], P. Loch[7], A. Loesle[50], T. Lohse[19], K. Lohwasser[146], M. Lokajicek[137], B.A. Long[25], J.D. Long[170], R.E. Long[87], L. Longo[65a,65b], K.A. Looper[122], J.A. Lopez[144b], I. Lopez Paz[14], A. Lopez Solis[146], J. Lorenz[112], N. Lorenzo Martinez[5], M. Losada[22], P.J. Lösel[112], X. Lou[44], X. Lou[15a], A. Lounis[128], J. Love[6], P.A. Love[87], J.J. Lozano Bahilo[171], H. Lu[61a], M. Lu[58a], N. Lu[103], Y.J. Lu[62], H.J. Lubatti[145], C. Luci[70a,70b], A. Lucotte[56], C. Luedtke[50], F. Luehring[63], I. Luise[132], L. Luminari[70a], B. Lund-Jensen[151], M.S. Lutz[100], P.M. Luzi[132], D. Lynn[29], R. Lysak[137], E. Lytken[94], F. Lyu[15a], V. Lyubushkin[77], H. Ma[29], L.L. Ma[58b], Y. Ma[58b], G. Maccarrone[49], A. Macchiolo[113], C.M. Macdonald[146], J. Machado Miguens[133,136b], D. Madaffari[171], R. Madar[37], W.F. Mader[46], A. Madsen[44], N. Madysa[46], J. Maeda[80], K. Maekawa[160], S. Maeland[17], T. Maeno[29], A.S. Maevskiy[111], V. Magerl[50], C. Maidantchik[78b], T. Maier[112], A. Maio[136a,136b,136d], O. Majersky[28a], S. Majewski[127], Y. Makida[79], N. Makovec[128], B. Malaescu[132], Pa. Malecki[82], V.P. Maleev[134], F. Malek[56], U. Mallik[75], D. Malon[6], C. Malone[31], S. Maltezos[10], S. Malyukov[35], J. Mamuzic[171], G. Mancini[49], I. Mandić[89], J. Maneira[136a], L. Manhaes de Andrade Filho[78a], J. Manjarres Ramos[46], K.H. Mankinen[94], A. Mann[112], A. Manousos[74], B. Mansoulie[142], J.D. Mansour[15a], M. Mantoani[51], S. Manzoni[66a,66b], G. Marceca[30], L. March[52], L. Marchese[131], G. Marchiori[132], M. Marcisovsky[137], C.A. Marin Tobon[35], M. Marjanovic[37], D.E. Marley[103], F. Marroquim[78b], Z. Marshall[18], M.U.F Martensson[169], S. Marti-Garcia[171], C.B. Martin[122], T.A. Martin[175], V.J. Martin[48], B. Martin dit Latour[17], M. Martinez[14,z], V.I. Martinez Outschoorn[100], S. Martin-Haugh[141], V.S. Martoiu[27b], A.C. Martyniuk[92], A. Marzin[35], L. Masetti[97], T. Mashimo[160], R. Mashinistov[108], J. Masik[98], A.L. Maslennikov[120b,120a], L.H. Mason[102], L. Massa[71a,71b], P. Massarotti[67a,67b], P. Mastrandrea[5], A. Mastroberardino[40b,40a], T. Masubuchi[160], P. Mättig[179], J. Maurer[27b], B. Maček[89], S.J. Maxfield[88], D.A. Maximov[120b,120a], R. Mazini[155], I. Maznas[159], S.M. Mazza[143], N.C. Mc Fadden[116], G. Mc Goldrick[164], S.P. Mc Kee[103], A. McCarn[103], T.G. McCarthy[113], L.I. McClymont[92], E.F. McDonald[102], J.A. Mcfayden[35], G. Mchedlidze[51], M.A. McKay[41], K.D. McLean[173], S.J. McMahon[141], P.C. McNamara[102], C.J. McNicol[175], R.A. McPherson[173,ad], J.E. Mdhluli[32c], Z.A. Meadows[100], S. Meehan[145], T.M. Megy[50], S. Mehlhase[112], A. Mehta[88], T. Meideck[56], B. Meirose[42], D. Melini[171,h], B.R. Mellado Garcia[32c], J.D. Mellenthin[51], M. Melo[28a], F. Meloni[44], A. Melzer[24], S.B. Menary[98], E.D. Mendes Gouveia[136a], L. Meng[88], X.T. Meng[103], A. Mengarelli[23b,23a], S. Menke[113], E. Meoni[40b,40a], S. Mergelmeyer[19], C. Merlassino[20], P. Mermod[52], L. Merola[67a,67b], C. Meroni[66a], F.S. Merritt[36], A. Messina[70a,70b], J. Metcalfe[6], A.S. Mete[168], C. Meyer[133], J. Meyer[157], J-P. Meyer[142], H. Meyer Zu Theenhausen[59a], F. Miano[153], R.P. Middleton[141], L. Mijović[48], G. Mikenberg[177], M. Mikestikova[137], M. Mikuž[89], M. Milesi[102], A. Milic[164], D.A. Millar[90], D.W. Miller[36], A. Milov[177], D.A. Milstead[43a,43b],

A.A. Minaenko[140], M. Miñano Moya[171], I.A. Minashvili[156b], A.I. Mincer[121], B. Mindur[81a], M. Mineev[77], Y. Minegishi[160], Y. Ming[178], L.M. Mir[14], A. Mirto[65a,65b], K.P. Mistry[133], T. Mitani[176], J. Mitrevski[112], V.A. Mitsou[171], A. Miucci[20], P.S. Miyagawa[146], A. Mizukami[79], J.U. Mjörnmark[94], T. Mkrtchyan[181], M. Mlynarikova[139], T. Moa[43a,43b], K. Mochizuki[107], P. Mogg[50], S. Mohapatra[38], S. Molander[43a,43b], R. Moles-Valls[24], M.C. Mondragon[104], K. Mönig[44], J. Monk[39], E. Monnier[99], A. Montalbano[149], J. Montejo Berlingen[35], F. Monticelli[86], S. Monzani[66a], N. Morange[128], D. Moreno[22], M. Moreno Llácer[35], P. Morettini[53b], M. Morgenstern[118], S. Morgenstern[46], D. Mori[149], M. Morii[57], M. Morinaga[176], V. Morisbak[130], A.K. Morley[35], G. Mornacchi[35], A.P. Morris[92], J.D. Morris[90], L. Morvaj[152], P. Moschovakos[10], M. Mosidze[156b], H.J. Moss[146], J. Moss[150,n], K. Motohashi[162], R. Mount[150], E. Mountricha[35], E.J.W. Moyse[100], S. Muanza[99], F. Mueller[113], J. Mueller[135], R.S.P. Mueller[112], D. Muenstermann[87], G.A. Mullier[20], F.J. Munoz Sanchez[98], P. Murin[28b], W.J. Murray[175,141], A. Murrone[66a,66b], M. Muškinja[89], C. Mwewa[32a], A.G. Myagkov[140,al], J. Myers[127], M. Myska[138], B.P. Nachman[18], O. Nackenhorst[45], K. Nagai[131], K. Nagano[79], Y. Nagasaka[60], M. Nagel[50], E. Nagy[99], A.M. Nairz[35], Y. Nakahama[115], K. Nakamura[79], T. Nakamura[160], I. Nakano[123], H. Nanjo[129], F. Napolitano[59a], R.F. Naranjo Garcia[44], R. Narayan[11], D.I. Narrias Villar[59a], I. Naryshkin[134], T. Naumann[44], G. Navarro[22], R. Nayyar[7], H.A. Neal[103], P.Y. Nechaeva[108], T.J. Neep[142], A. Negri[68a,68b], M. Negrini[23b], S. Nektarijevic[117], C. Nellist[51], M.E. Nelson[131], S. Nemecek[137], P. Nemethy[121], M. Nessi[35,e], M.S. Neubauer[170], M. Neumann[179], P.R. Newman[21], T.Y. Ng[61c], Y.S. Ng[19], H.D.N. Nguyen[99], T. Nguyen Manh[107], E. Nibigira[37], R.B. Nickerson[131], R. Nicolaidou[142], J. Nielsen[143], N. Nikiforou[11], V. Nikolaenko[140,al], I. Nikolic-Audit[132], K. Nikolopoulos[21], P. Nilsson[29], Y. Ninomiya[79], A. Nisati[70a], N. Nishu[58c], R. Nisius[113], I. Nitsche[45], T. Nitta[176], T. Nobe[160], Y. Noguchi[83], M. Nomachi[129], I. Nomidis[132], M.A. Nomura[29], T. Nooney[90], M. Nordberg[35], N. Norjoharuddeen[131], T. Novak[89], O. Novgorodova[46], R. Novotny[138], L. Nozka[126], K. Ntekas[168], E. Nurse[92], F. Nuti[102], F.G. Oakham[33,as], H. Oberlack[113], T. Obermann[24], J. Ocariz[132], A. Ochi[80], I. Ochoa[38], J.P. Ochoa-Ricoux[144a], K. O'Connor[26], S. Oda[85], S. Odaka[79], S. Oerdek[51], A. Oh[98], S.H. Oh[47], C.C. Ohm[151], H. Oide[53b,53a], M.L. Ojeda[164], H. Okawa[166], Y. Okazaki[83], Y. Okumura[160], T. Okuyama[79], A. Olariu[27b], L.F. Oleiro Seabra[136a], S.A. Olivares Pino[144a], D. Oliveira Damazio[29], J.L. Oliver[1], M.J.R. Olsson[36], A. Olszewski[82], J. Olszowska[82], D.C. O'Neil[149], A. Onofre[136a,136e], K. Onogi[115], P.U.E. Onyisi[11], H. Oppen[130], M.J. Oreglia[36], G.E. Orellana[86], Y. Oren[158], D. Orestano[72a,72b], E.C. Orgill[98], N. Orlando[61b], A.A. O'Rourke[44], R.S. Orr[164], B. Osculati[53b,53a,*], V. O'Shea[55], R. Ospanov[58a], G. Otero y Garzon[30], H. Otono[85], M. Ouchrif[34d], F. Ould-Saada[130], A. Ouraou[142], Q. Ouyang[15a], M. Owen[55], R.E. Owen[21], V.E. Ozcan[12c], N. Ozturk[8], J. Pacalt[126], H.A. Pacey[31], K. Pachal[149], A. Pacheco Pages[14], L. Pacheco Rodriguez[142], C. Padilla Aranda[14], S. Pagan Griso[18], M. Paganini[180], G. Palacino[63], S. Palazzo[40b,40a], S. Palestini[35], M. Palka[81b], D. Pallin[37], I. Panagoulias[10], C.E. Pandini[35], J.G. Panduro Vazquez[91], P. Pani[35], G. Panizzo[64a,64c], L. Paolozzi[52], T.D. Papadopoulou[10], K. Papageorgiou[9,j], A. Paramonov[6], D. Paredes Hernandez[61b], S.R. Paredes Saenz[131], B. Parida[163], A.J. Parker[87], K.A. Parker[44], M.A. Parker[31], F. Parodi[53b,53a], J.A. Parsons[38], U. Parzefall[50], V.R. Pascuzzi[164], J.M.P. Pasner[143], E. Pasqualucci[70a], S. Passaggio[53b], F. Pastore[91], P. Pasuwan[43a,43b], S. Pataraia[97], J.R. Pater[98], A. Pathak[178,k], T. Pauly[35], B. Pearson[113], M. Pedersen[130], L. Pedraza Diaz[117], R. Pedro[136a,136b], S.V. Peleganchuk[120b,120a], O. Penc[137], C. Peng[15d], H. Peng[58a], B.S. Peralva[78a], M.M. Perego[142], A.P. Pereira Peixoto[136a], D.V. Perepelitsa[29], M. Perez-Victoria[g], F. Peri[19], L. Perini[66a,66b], H. Pernegger[35], S. Perrella[67a,67b], V.D. Peshekhonov[77,*], K. Peters[44], R.F.Y. Peters[98], B.A. Petersen[35], T.C. Petersen[39], E. Petit[56], A. Petridis[1], C. Petridou[159], P. Petroff[128], M. Petrov[131], F. Petrucci[72a,72b], M. Pettee[180], N.E. Pettersson[100], A. Peyaud[142], R. Pezoa[144b], T. Pham[102], F.H. Phillips[104], P.W. Phillips[141], M.W. Phipps[170], G. Piacquadio[152], E. Pianori[18], A. Picazio[100], M.A. Pickering[131], R.H. Pickles[98], R. Piegaia[30], J.E. Pilcher[36], A.D. Pilkington[98], M. Pinamonti[71a,71b], J.L. Pinfold[3], M. Pitt[177], M-A. Pleier[29], V. Pleskot[139],

E. Plotnikova[77], D. Pluth[76], P. Podberezko[120b,120a], R. Poettgen[94], R. Poggi[52], L. Poggioli[128], I. Pogrebnyak[104], D. Pohl[24], I. Pokharel[51], G. Polesello[68a], A. Poley[18], A. Policicchio[70a,70b], R. Polifka[35], A. Polini[23b], C.S. Pollard[44], V. Polychronakos[29], D. Ponomarenko[110], L. Pontecorvo[70a], G.A. Popeneciu[27d], D.M. Portillo Quintero[132], S. Pospisil[138], K. Potamianos[44], I.N. Potrap[77], C.J. Potter[31], H. Potti[11], T. Poulsen[94], J. Poveda[35], T.D. Powell[146], M.E. Pozo Astigarraga[35], P. Pralavorio[99], S. Prell[76], D. Price[98], M. Primavera[65a], S. Prince[101], N. Proklova[110], K. Prokofiev[61c], F. Prokoshin[144b], S. Protopopescu[29], J. Proudfoot[6], M. Przybycien[81a], A. Puri[170], P. Puzo[128], J. Qian[103], Y. Qin[98], A. Quadt[51], M. Queitsch-Maitland[44], A. Qureshi[1], P. Rados[102], F. Ragusa[66a,66b], G. Rahal[95], J.A. Raine[52], S. Rajagopalan[29], A. Ramirez Morales[90], T. Rashid[128], S. Raspopov[5], M.G. Ratti[66a,66b], D.M. Rauch[44], F. Rauscher[112], S. Rave[97], B. Ravina[146], I. Ravinovich[177], J.H. Rawling[98], M. Raymond[35], A.L. Read[130], N.P. Readioff[56], M. Reale[65a,65b], D.M. Rebuzzi[68a,68b], A. Redelbach[174], G. Redlinger[29], R. Reece[143], R.G. Reed[32c], K. Reeves[42], L. Rehnisch[19], J. Reichert[133], D. Reikher[158], A. Reiss[97], C. Rembser[35], H. Ren[15d], M. Rescigno[70a], S. Resconi[66a], E.D. Resseguie[133], S. Rettie[172], E. Reynolds[21], O.L. Rezanova[120b,120a], P. Reznicek[139], E. Ricci[73a,73b], R. Richter[113], S. Richter[44], E. Richter-Was[81b], O. Ricken[24], M. Ridel[132], P. Rieck[113], C.J. Riegel[179], O. Rifki[44], M. Rijssenbeek[152], A. Rimoldi[68a,68b], M. Rimoldi[20], L. Rinaldi[23b], G. Ripellino[151], B. Ristić[87], E. Ritsch[35], I. Riu[14], J.C. Rivera Vergara[144a], F. Rizatdinova[125], E. Rizvi[90], C. Rizzi[14], R.T. Roberts[98], S.H. Robertson[101,ad], D. Robinson[31], J.E.M. Robinson[44], A. Robson[55], E. Rocco[97], C. Roda[69a,69b], Y. Rodina[99], S. Rodriguez Bosca[171], A. Rodriguez Perez[14], D. Rodriguez Rodriguez[171], A.M. Rodríguez Vera[165b], S. Roe[35], C.S. Rogan[57], O. Røhne[130], R. Röhrig[113], C.P.A. Roland[63], J. Roloff[57], A. Romaniouk[110], M. Romano[23b,23a], N. Rompotis[88], M. Ronzani[121], L. Roos[132], S. Rosati[70a], K. Rosbach[50], P. Rose[143], N-A. Rosien[51], E. Rossi[44], E. Rossi[72a,72b], E. Rossi[67a,67b], L.P. Rossi[53b], L. Rossini[66a,66b], J.H.N. Rosten[31], R. Rosten[14], M. Rotaru[27b], J. Rothberg[145], D. Rousseau[128], D. Roy[32c], A. Rozanov[99], Y. Rozen[157], X. Ruan[32c], F. Rubbo[150], F. Rühr[50], A. Ruiz-Martinez[171], Z. Rurikova[50], N.A. Rusakovich[77], H.L. Russell[101], J.P. Rutherfoord[7], E.M. Rüttinger[44,l], Y.F. Ryabov[134], M. Rybar[170], G. Rybkin[128], S. Ryu[6], A. Ryzhov[140], G.F. Rzehorz[51], P. Sabatini[51], G. Sabato[118], S. Sacerdoti[128], H.F-W. Sadrozinski[143], R. Sadykov[77], F. Safai Tehrani[70a], P. Saha[119], M. Sahinsoy[59a], A. Sahu[179], M. Saimpert[44], M. Saito[160], T. Saito[160], H. Sakamoto[160], A. Sakharov[121,ak], D. Salamani[52], G. Salamanna[72a,72b], J.E. Salazar Loyola[144b], D. Salek[118], P.H. Sales De Bruin[169], D. Salihagic[113], A. Salnikov[150], J. Salt[171], D. Salvatore[40b,40a], F. Salvatore[153], A. Salvucci[61a,61b,61c], A. Salzburger[35], J. Samarati[35], D. Sammel[50], D. Sampsonidis[159], D. Sampsonidou[159], J. Sánchez[171], A. Sanchez Pineda[64a,64c], H. Sandaker[130], C.O. Sander[44], M. Sandhoff[179], C. Sandoval[22], D.P.C. Sankey[141], M. Sannino[53b,53a], Y. Sano[115], A. Sansoni[49], C. Santoni[37], H. Santos[136a], I. Santoyo Castillo[153], A. Santra[171], A. Sapronov[77], J.G. Saraiva[136a,136d], O. Sasaki[79], K. Sato[166], E. Sauvan[5], P. Savard[164,as], N. Savic[113], R. Sawada[160], C. Sawyer[141], L. Sawyer[93,aj], C. Sbarra[23b], A. Sbrizzi[23b,23a], T. Scanlon[92], J. Schaarschmidt[145], P. Schacht[113], B.M. Schachtner[112], D. Schaefer[36], L. Schaefer[133], J. Schaeffer[97], S. Schaepe[35], U. Schäfer[97], A.C. Schaffer[128], D. Schaile[112], R.D. Schamberger[152], N. Scharmberg[98], V.A. Schegelsky[134], D. Scheirich[139], F. Schenck[19], M. Schernau[168], C. Schiavi[53b,53a], S. Schier[143], L.K. Schildgen[24], Z.M. Schillaci[26], E.J. Schioppa[35], M. Schioppa[40b,40a], K.E. Schleicher[50], S. Schlenker[35], K.R. Schmidt-Sommerfeld[113], K. Schmieden[35], C. Schmitt[97], S. Schmitt[44], S. Schmitz[97], J.C. Schmoeckel[44], U. Schnoor[50], L. Schoeffel[142], A. Schoening[59b], E. Schopf[24], M. Schott[97], J.F.P. Schouwenberg[117], J. Schovancova[35], S. Schramm[52], A. Schulte[97], H-C. Schultz-Coulon[59a], M. Schumacher[50], B.A. Schumm[143], Ph. Schune[142], A. Schwartzman[150], T.A. Schwarz[103], Ph. Schwemling[142], R. Schwienhorst[104], A. Sciandra[24], G. Sciolla[26], M. Scornajenghi[40b,40a], F. Scuri[69a], F. Scutti[102], L.M. Scyboz[113], J. Searcy[103], C.D. Sebastiani[70a,70b], P. Seema[19], S.C. Seidel[116], A. Seiden[143], T. Seiss[36], J.M. Seixas[78b], G. Sekhniaidze[67a], K. Sekhon[103], S.J. Sekula[41], N. Semprini-Cesari[23b,23a], S. Sen[47], S. Senkin[37], C. Serfon[130], L. Serin[128], L. Serkin[64a,64b], M. Sessa[58a],

H. Severini[124], F. Sforza[167], A. Sfyrla[52], E. Shabalina[51], J.D. Shahinian[143], N.W. Shaikh[43a,43b], L.Y. Shan[15a], R. Shang[170], J.T. Shank[25], M. Shapiro[18], A.S. Sharma[1], A. Sharma[131], P.B. Shatalov[109], K. Shaw[153], S.M. Shaw[98], A. Shcherbakova[134], Y. Shen[124], N. Sherafati[33], A.D. Sherman[25], P. Sherwood[92], L. Shi[155,ao], S. Shimizu[79], C.O. Shimmin[180], M. Shimojima[114], I.P.J. Shipsey[131], S. Shirabe[85], M. Shiyakova[77], J. Shlomi[177], A. Shmeleva[108], D. Shoaleh Saadi[107], M.J. Shochet[36], S. Shojaii[102], D.R. Shope[124], S. Shrestha[122], E. Shulga[110], P. Sicho[137], A.M. Sickles[170], P.E. Sidebo[151], E. Sideras Haddad[32c], O. Sidiropoulou[35], A. Sidoti[23b,23a], F. Siegert[46], Dj. Sijacki[16], J. Silva[136a], M. Silva Jr.[178], M.V. Silva Oliveira[78a], S.B. Silverstein[43a], L. Simic[77], S. Simion[128], E. Simioni[97], M. Simon[97], R. Simoniello[97], P. Sinervo[164], N.B. Sinev[127], M. Sioli[23b,23a], G. Siragusa[174], I. Siral[103], S.Yu. Sivoklokov[111], J. Sjölin[43a,43b], P. Skubic[124], M. Slater[21], T. Slavicek[138], M. Slawinska[82], K. Sliwa[167], R. Slovak[139], V. Smakhtin[177], B.H. Smart[5], J. Smiesko[28a], N. Smirnov[110], S.Yu. Smirnov[110], Y. Smirnov[110], L.N. Smirnova[111], O. Smirnova[94], J.W. Smith[51], M.N.K. Smith[38], M. Smizanska[87], K. Smolek[138], A. Smykiewicz[82], A.A. Snesarev[108], I.M. Snyder[127], S. Snyder[29], R. Sobie[173,ad], A.M. Soffa[168], A. Soffer[158], A. Søgaard[48], D.A. Soh[155], G. Sokhrannyi[89], C.A. Solans Sanchez[35], M. Solar[138], E.Yu. Soldatov[110], U. Soldevila[171], A.A. Solodkov[140], A. Soloshenko[77], O.V. Solovyanov[140], V. Solovyev[134], P. Sommer[146], H. Son[167], W. Song[141], W.Y. Song[165b], A. Sopczak[138], F. Sopkova[28b], C.L. Sotiropoulou[69a,69b], S. Sottocornola[68a,68b], R. Soualah[64a,64c,i], A.M. Soukharev[120b,120a], D. South[44], B.C. Sowden[91], S. Spagnolo[65a,65b], M. Spalla[113], M. Spangenberg[175], F. Spanò[91], D. Sperlich[19], F. Spettel[113], T.M. Spieker[59a], R. Spighi[23b], G. Spigo[35], L.A. Spiller[102], D.P. Spiteri[55], M. Spousta[139], A. Stabile[66a,66b], R. Stamen[59a], S. Stamm[19], E. Stanecka[82], R.W. Stanek[6], C. Stanescu[72a], B. Stanislaus[131], M.M. Stanitzki[44], B. Stapf[118], S. Stapnes[130], E.A. Starchenko[140], G.H. Stark[36], J. Stark[56], S.H Stark[39], P. Staroba[137], P. Starovoitov[59a], S. Stärz[35], R. Staszewski[82], M. Stegler[44], P. Steinberg[29], B. Stelzer[149], H.J. Stelzer[35], O. Stelzer-Chilton[165a], H. Stenzel[54], T.J. Stevenson[90], G.A. Stewart[55], M.C. Stockton[127], G. Stoicea[27b], P. Stolte[51], S. Stonjek[113], A. Straessner[46], J. Strandberg[151], S. Strandberg[43a,43b], M. Strauss[124], P. Strizenec[28b], R. Ströhmer[174], D.M. Strom[127], R. Stroynowski[41], A. Strubig[48], S.A. Stucci[29], B. Stugu[17], J. Stupak[124], N.A. Styles[44], D. Su[150], J. Su[135], S. Suchek[59a], Y. Sugaya[129], M. Suk[138], V.V. Sulin[108], M.J. Sullivan[88], D.M.S. Sultan[52], S. Sultansoy[4c], T. Sumida[83], S. Sun[103], X. Sun[3], K. Suruliz[153], C.J.E. Suster[154], M.R. Sutton[153], S. Suzuki[79], M. Svatos[137], M. Swiatlowski[36], S.P. Swift[2], A. Sydorenko[97], I. Sykora[28a], T. Sykora[139], D. Ta[97], K. Tackmann[44,aa], J. Taenzer[158], A. Taffard[168], R. Tafirout[165a], E. Tahirovic[90], N. Taiblum[158], H. Takai[29], R. Takashima[84], E.H. Takasugi[113], K. Takeda[80], T. Takeshita[147], Y. Takubo[79], M. Talby[99], A.A. Talyshev[120b,120a], J. Tanaka[160], M. Tanaka[162], R. Tanaka[128], B.B. Tannenwald[122], S. Tapia Araya[144b], S. Tapprogge[97], A. Tarek Abouelfadl Mohamed[132], S. Tarem[157], G. Tarna[27b,d], G.F. Tartarelli[66a], P. Tas[139], M. Tasevsky[137], T. Tashiro[83], E. Tassi[40b,40a], A. Tavares Delgado[136a,136b], Y. Tayalati[34e], A.C. Taylor[116], A.J. Taylor[48], G.N. Taylor[102], P.T.E. Taylor[102], W. Taylor[165b], A.S. Tee[87], P. Teixeira-Dias[91], H. Ten Kate[35], P.K. Teng[155], J.J. Teoh[118], S. Terada[79], K. Terashi[160], J. Terron[96], S. Terzo[14], M. Testa[49], R.J. Teuscher[164,ad], S.J. Thais[180], T. Theveneaux-Pelzer[44], F. Thiele[39], D.W. Thomas[91], J.P. Thomas[21], A.S. Thompson[55], P.D. Thompson[21], L.A. Thomsen[180], E. Thomson[133], Y. Tian[38], R.E. Ticse Torres[51], V.O. Tikhomirov[108,am], Yu.A. Tikhonov[120b,120a], S. Timoshenko[110], P. Tipton[180], S. Tisserant[99], K. Todome[162], S. Todorova-Nova[5], S. Todt[46], J. Tojo[85], S. Tokár[28a], K. Tokushuku[79], E. Tolley[122], K.G. Tomiwa[32c], M. Tomoto[115], L. Tompkins[150,q], K. Toms[116], B. Tong[57], P. Tornambe[50], E. Torrence[127], H. Torres[46], E. Torró Pastor[145], C. Tosciri[131], J. Toth[99,ac], F. Touchard[99], D.R. Tovey[146], C.J. Treado[121], T. Trefzger[174], F. Tresoldi[153], A. Tricoli[29], I.M. Trigger[165a], S. Trincaz-Duvoid[132], M.F. Tripiana[14], W. Trischuk[164], B. Trocmé[56], A. Trofymov[128], C. Troncon[66a], M. Trovatelli[173], F. Trovato[153], L. Truong[32b], M. Trzebinski[82], A. Trzupek[82], F. Tsai[44], J.C-L. Tseng[131], P.V. Tsiareshka[105], A. Tsirigotis[159], N. Tsirintanis[9], V. Tsiskaridze[152], E.G. Tskhadadze[156a], I.I. Tsukerman[109], V. Tsulaia[18], S. Tsuno[79], D. Tsybychev[152,163], Y. Tu[61b], A. Tudorache[27b],

V. Tudorache[27b], T.T. Tulbure[27a], A.N. Tuna[57], S. Turchikhin[77], D. Turgeman[177], I. Turk Cakir[4b,u], R. Turra[66a], P.M. Tuts[38], E. Tzovara[97], G. Ucchielli[23b,23a], I. Ueda[79], M. Ughetto[43a,43b], F. Ukegawa[166], G. Unal[35], A. Undrus[29], G. Unel[168], F.C. Ungaro[102], Y. Unno[79], K. Uno[160], J. Urban[28b], P. Urquijo[102], P. Urrejola[97], G. Usai[8], J. Usui[79], L. Vacavant[99], V. Vacek[138], B. Vachon[101], K.O.H. Vadla[130], A. Vaidya[92], C. Valderanis[112], E. Valdes Santurio[43a,43b], M. Valente[52], S. Valentinetti[23b,23a], A. Valero[171], L. Valéry[44], R.A. Vallance[21], A. Vallier[5], J.A. Valls Ferrer[171], T.R. Van Daalen[14], H. Van der Graaf[118], P. Van Gemmeren[6], J. Van Nieuwkoop[149], I. Van Vulpen[118], M. Vanadia[71a,71b], W. Vandelli[35], A. Vaniachine[163], P. Vankov[118], R. Vari[70a], E.W. Varnes[7], C. Varni[53b,53a], T. Varol[41], D. Varouchas[128], K.E. Varvell[154], G.A. Vasquez[144b], J.G. Vasquez[180], F. Vazeille[37], D. Vazquez Furelos[14], T. Vazquez Schroeder[101], J. Veatch[51], V. Vecchio[72a,72b], L.M. Veloce[164], F. Veloso[136a,136c], S. Veneziano[70a], A. Ventura[65a,65b], M. Venturi[173], N. Venturi[35], V. Vercesi[68a], M. Verducci[72a,72b], C.M. Vergel Infante[76], C. Vergis[24], W. Verkerke[118], A.T. Vermeulen[118], J.C. Vermeulen[118], M.C. Vetterli[149,as], N. Viaux Maira[144b], M. Vicente Barreto Pinto[52], I. Vichou[170,*], T. Vickey[146], O.E. Vickey Boeriu[146], G.H.A. Viehhauser[131], S. Viel[18], L. Vigani[131], M. Villa[23b,23a], M. Villaplana Perez[66a,66b], E. Vilucchi[49], M.G. Vincter[33], V.B. Vinogradov[77], A. Vishwakarma[44], C. Vittori[23b,23a], I. Vivarelli[153], S. Vlachos[10], M. Vogel[179], P. Vokac[138], G. Volpi[14], S.E. von Buddenbrock[32c], E. Von Toerne[24], V. Vorobel[139], K. Vorobev[110], M. Vos[171], J.H. Vossebeld[88], N. Vranjes[16], M. Vranjes Milosavljevic[16], V. Vrba[138], M. Vreeswijk[118], T. Šfiligoj[89], R. Vuillermet[35], I. Vukotic[36], T. Ženiš[28a], L. Živković[16], P. Wagner[24], W. Wagner[179], J. Wagner-Kuhr[112], H. Wahlberg[86], S. Wahrmund[46], K. Wakamiya[80], V.M. Walbrecht[113], J. Walder[87], R. Walker[112], S.D. Walker[91], W. Walkowiak[148], V. Wallangen[43a,43b], A.M. Wang[57], C. Wang[58b,d], F. Wang[178], H. Wang[18], H. Wang[3], J. Wang[154], J. Wang[59b], P. Wang[41], Q. Wang[124], R.-J. Wang[132], R. Wang[58a], R. Wang[6], S.M. Wang[155], W.T. Wang[58a], W. Wang[15c,ae], W.X. Wang[58a,ae], Y. Wang[58a], Z. Wang[58c], C. Wanotayaroj[44], A. Warburton[101], C.P. Ward[31], D.R. Wardrope[92], A. Washbrook[48], P.M. Watkins[21], A.T. Watson[21], M.F. Watson[21], G. Watts[145], S. Watts[98], B.M. Waugh[92], A.F. Webb[11], S. Webb[97], C. Weber[180], M.S. Weber[20], S.A. Weber[33], S.M. Weber[59a], A.R. Weidberg[131], B. Weinert[63], J. Weingarten[45], M. Weirich[97], C. Weiser[50], P.S. Wells[35], T. Wenaus[29], T. Wengler[35], S. Wenig[35], N. Wermes[24], M.D. Werner[76], P. Werner[35], M. Wessels[59a], T.D. Weston[20], K. Whalen[127], N.L. Whallon[145], A.M. Wharton[87], A.S. White[103], A. White[8], M.J. White[1], R. White[144b], D. Whiteson[168], B.W. Whitmore[87], F.J. Wickens[141], W. Wiedenmann[178], M. Wielers[141], C. Wiglesworth[39], L.A.M. Wiik-Fuchs[50], A. Wildauer[113], F. Wilk[98], H.G. Wilkens[35], L.J. Wilkins[91], H.H. Williams[133], S. Williams[31], C. Willis[104], S. Willocq[100], J.A. Wilson[21], I. Wingerter-Seez[5], E. Winkels[153], F. Winklmeier[127], O.J. Winston[153], B.T. Winter[24], M. Wittgen[150], M. Wobisch[93], A. Wolf[97], T.M.H. Wolf[118], R. Wolff[99], M.W. Wolter[82], H. Wolters[136a,136c], V.W.S. Wong[172], N.L. Woods[143], S.D. Worm[21], B.K. Wosiek[82], K.W. Woźniak[82], K. Wraight[55], M. Wu[36], S.L. Wu[178], X. Wu[52], Y. Wu[58a], T.R. Wyatt[98], B.M. Wynne[48], S. Xella[39], Z. Xi[103], L. Xia[175], D. Xu[15a], H. Xu[58a], L. Xu[29], T. Xu[142], W. Xu[103], B. Yabsley[154], S. Yacoob[32a], K. Yajima[129], D.P. Yallup[92], D. Yamaguchi[162], Y. Yamaguchi[162], A. Yamamoto[79], T. Yamanaka[160], F. Yamane[80], M. Yamatani[160], T. Yamazaki[160], Y. Yamazaki[80], Z. Yan[25], H.J. Yang[58c,58d], H.T. Yang[18], S. Yang[75], Y. Yang[160], Z. Yang[17], W-M. Yao[18], Y.C. Yap[44], Y. Yasu[79], E. Yatsenko[58c,58d], J. Ye[41], S. Ye[29], I. Yeletskikh[77], E. Yigitbasi[25], E. Yildirim[97], K. Yorita[176], K. Yoshihara[133], C.J.S. Young[35], C. Young[150], J. Yu[8], J. Yu[76], X. Yue[59a], S.P.Y. Yuen[24], B. Zabinski[82], G. Zacharis[10], E. Zaffaroni[52], R. Zaidan[14], A.M. Zaitsev[140,al], T. Zakareishvili[156b], N. Zakharchuk[33], J. Zalieckas[17], S. Zambito[57], D. Zanzi[35], D.R. Zaripovas[55], S.V. Zeißner[45], C. Zeitnitz[179], G. Zemaityte[131], J.C. Zeng[170], Q. Zeng[150], O. Zenin[140], D. Zerwas[128], M. Zgubič[131], D.F. Zhang[58b], D. Zhang[103], F. Zhang[178], G. Zhang[58a], H. Zhang[15c], J. Zhang[6], L. Zhang[15c], L. Zhang[58a], M. Zhang[170], P. Zhang[15c], R. Zhang[58a], R. Zhang[24], X. Zhang[58b], Y. Zhang[15d], Z. Zhang[128], P. Zhao[47], X. Zhao[41], Y. Zhao[58b,128,ai], Z. Zhao[58a], A. Zhemchugov[77], D. Zhong[170], B. Zhou[103], C. Zhou[178], L. Zhou[41],

M.S. Zhou[15d], M. Zhou[152], N. Zhou[58c], Y. Zhou[7], C.G. Zhu[58b], H.L. Zhu[58a], H. Zhu[15a], J. Zhu[103], Y. Zhu[58a], X. Zhuang[15a], K. Zhukov[108], V. Zhulanov[120b,120a], A. Zibell[174], D. Zieminska[63], N.I. Zimine[77], S. Zimmermann[50], Z. Zinonos[113], M. Zinser[97], M. Ziolkowski[148], G. Zobernig[178], A. Zoccoli[23b,23a], K. Zoch[51], T.G. Zorbas[146], R. Zou[36], M. Zur Nedden[19], L. Zwalinski[35].

[1]Department of Physics, University of Adelaide, Adelaide; Australia.
[2]Physics Department, SUNY Albany, Albany NY; United States of America.
[3]Department of Physics, University of Alberta, Edmonton AB; Canada.
[4(a)]Department of Physics, Ankara University, Ankara;[(b)]Istanbul Aydin University, Istanbul;[(c)]Division of Physics, TOBB University of Economics and Technology, Ankara; Turkey.
[5]LAPP, Université Grenoble Alpes, Université Savoie Mont Blanc, CNRS/IN2P3, Annecy; France.
[6]High Energy Physics Division, Argonne National Laboratory, Argonne IL; United States of America.
[7]Department of Physics, University of Arizona, Tucson AZ; United States of America.
[8]Department of Physics, University of Texas at Arlington, Arlington TX; United States of America.
[9]Physics Department, National and Kapodistrian University of Athens, Athens; Greece.
[10]Physics Department, National Technical University of Athens, Zografou; Greece.
[11]Department of Physics, University of Texas at Austin, Austin TX; United States of America.
[12(a)]Bahcesehir University, Faculty of Engineering and Natural Sciences, Istanbul;[(b)]Istanbul Bilgi University, Faculty of Engineering and Natural Sciences, Istanbul;[(c)]Department of Physics, Bogazici University, Istanbul;[(d)]Department of Physics Engineering, Gaziantep University, Gaziantep; Turkey.
[13]Institute of Physics, Azerbaijan Academy of Sciences, Baku; Azerbaijan.
[14]Institut de Física d'Altes Energies (IFAE), Barcelona Institute of Science and Technology, Barcelona; Spain.
[15(a)]Institute of High Energy Physics, Chinese Academy of Sciences, Beijing;[(b)]Physics Department, Tsinghua University, Beijing;[(c)]Department of Physics, Nanjing University, Nanjing;[(d)]University of Chinese Academy of Science (UCAS), Beijing; China.
[16]Institute of Physics, University of Belgrade, Belgrade; Serbia.
[17]Department for Physics and Technology, University of Bergen, Bergen; Norway.
[18]Physics Division, Lawrence Berkeley National Laboratory and University of California, Berkeley CA; United States of America.
[19]Institut für Physik, Humboldt Universität zu Berlin, Berlin; Germany.
[20]Albert Einstein Center for Fundamental Physics and Laboratory for High Energy Physics, University of Bern, Bern; Switzerland.
[21]School of Physics and Astronomy, University of Birmingham, Birmingham; United Kingdom.
[22]Centro de Investigaciónes, Universidad Antonio Nariño, Bogota; Colombia.
[23(a)]Dipartimento di Fisica e Astronomia, Università di Bologna, Bologna;[(b)]INFN Sezione di Bologna; Italy.
[24]Physikalisches Institut, Universität Bonn, Bonn; Germany.
[25]Department of Physics, Boston University, Boston MA; United States of America.
[26]Department of Physics, Brandeis University, Waltham MA; United States of America.
[27(a)]Transilvania University of Brasov, Brasov;[(b)]Horia Hulubei National Institute of Physics and Nuclear Engineering, Bucharest;[(c)]Department of Physics, Alexandru Ioan Cuza University of Iasi, Iasi;[(d)]National Institute for Research and Development of Isotopic and Molecular Technologies, Physics Department, Cluj-Napoca;[(e)]University Politehnica Bucharest, Bucharest;[(f)]West University in Timisoara, Timisoara; Romania.
[28(a)]Faculty of Mathematics, Physics and Informatics, Comenius University, Bratislava;[(b)]Department of Subnuclear Physics, Institute of Experimental Physics of the Slovak Academy of Sciences, Kosice;

Slovak Republic.
[29]Physics Department, Brookhaven National Laboratory, Upton NY; United States of America.
[30]Departamento de Física, Universidad de Buenos Aires, Buenos Aires; Argentina.
[31]Cavendish Laboratory, University of Cambridge, Cambridge; United Kingdom.
[32(a)]Department of Physics, University of Cape Town, Cape Town;[(b)]Department of Mechanical Engineering Science, University of Johannesburg, Johannesburg;[(c)]School of Physics, University of the Witwatersrand, Johannesburg; South Africa.
[33]Department of Physics, Carleton University, Ottawa ON; Canada.
[34(a)]Faculté des Sciences Ain Chock, Réseau Universitaire de Physique des Hautes Energies - Université Hassan II, Casablanca;[(b)]Centre National de l'Energie des Sciences Techniques Nucleaires (CNESTEN), Rabat;[(c)]Faculté des Sciences Semlalia, Université Cadi Ayyad, LPHEA-Marrakech;[(d)]Faculté des Sciences, Université Mohamed Premier and LPTPM, Oujda;[(e)]Faculté des sciences, Université Mohammed V, Rabat; Morocco.
[35]CERN, Geneva; Switzerland.
[36]Enrico Fermi Institute, University of Chicago, Chicago IL; United States of America.
[37]LPC, Université Clermont Auvergne, CNRS/IN2P3, Clermont-Ferrand; France.
[38]Nevis Laboratory, Columbia University, Irvington NY; United States of America.
[39]Niels Bohr Institute, University of Copenhagen, Copenhagen; Denmark.
[40(a)]Dipartimento di Fisica, Università della Calabria, Rende;[(b)]INFN Gruppo Collegato di Cosenza, Laboratori Nazionali di Frascati; Italy.
[41]Physics Department, Southern Methodist University, Dallas TX; United States of America.
[42]Physics Department, University of Texas at Dallas, Richardson TX; United States of America.
[43(a)]Department of Physics, Stockholm University;[(b)]Oskar Klein Centre, Stockholm; Sweden.
[44]Deutsches Elektronen-Synchrotron DESY, Hamburg and Zeuthen; Germany.
[45]Lehrstuhl für Experimentelle Physik IV, Technische Universität Dortmund, Dortmund; Germany.
[46]Institut für Kern- und Teilchenphysik, Technische Universität Dresden, Dresden; Germany.
[47]Department of Physics, Duke University, Durham NC; United States of America.
[48]SUPA - School of Physics and Astronomy, University of Edinburgh, Edinburgh; United Kingdom.
[49]INFN e Laboratori Nazionali di Frascati, Frascati; Italy.
[50]Physikalisches Institut, Albert-Ludwigs-Universität Freiburg, Freiburg; Germany.
[51]II. Physikalisches Institut, Georg-August-Universität Göttingen, Göttingen; Germany.
[52]Département de Physique Nucléaire et Corpusculaire, Université de Genève, Genève; Switzerland.
[53(a)]Dipartimento di Fisica, Università di Genova, Genova;[(b)]INFN Sezione di Genova; Italy.
[54]II. Physikalisches Institut, Justus-Liebig-Universität Giessen, Giessen; Germany.
[55]SUPA - School of Physics and Astronomy, University of Glasgow, Glasgow; United Kingdom.
[56]LPSC, Université Grenoble Alpes, CNRS/IN2P3, Grenoble INP, Grenoble; France.
[57]Laboratory for Particle Physics and Cosmology, Harvard University, Cambridge MA; United States of America.
[58(a)]Department of Modern Physics and State Key Laboratory of Particle Detection and Electronics, University of Science and Technology of China, Hefei;[(b)]Institute of Frontier and Interdisciplinary Science and Key Laboratory of Particle Physics and Particle Irradiation (MOE), Shandong University, Qingdao;[(c)]School of Physics and Astronomy, Shanghai Jiao Tong University, KLPPAC-MoE, SKLPPC, Shanghai;[(d)]Tsung-Dao Lee Institute, Shanghai; China.
[59(a)]Kirchhoff-Institut für Physik, Ruprecht-Karls-Universität Heidelberg, Heidelberg;[(b)]Physikalisches Institut, Ruprecht-Karls-Universität Heidelberg, Heidelberg; Germany.
[60]Faculty of Applied Information Science, Hiroshima Institute of Technology, Hiroshima; Japan.
[61(a)]Department of Physics, Chinese University of Hong Kong, Shatin, N.T., Hong Kong;[(b)]Department

of Physics, University of Hong Kong, Hong Kong;[(c)]Department of Physics and Institute for Advanced Study, Hong Kong University of Science and Technology, Clear Water Bay, Kowloon, Hong Kong; China.
[62]Department of Physics, National Tsing Hua University, Hsinchu; Taiwan.
[63]Department of Physics, Indiana University, Bloomington IN; United States of America.
[64(a)]INFN Gruppo Collegato di Udine, Sezione di Trieste, Udine;[(b)]ICTP, Trieste;[(c)]Dipartimento di Chimica, Fisica e Ambiente, Università di Udine, Udine; Italy.
[65(a)]INFN Sezione di Lecce;[(b)]Dipartimento di Matematica e Fisica, Università del Salento, Lecce; Italy.
[66(a)]INFN Sezione di Milano;[(b)]Dipartimento di Fisica, Università di Milano, Milano; Italy.
[67(a)]INFN Sezione di Napoli;[(b)]Dipartimento di Fisica, Università di Napoli, Napoli; Italy.
[68(a)]INFN Sezione di Pavia;[(b)]Dipartimento di Fisica, Università di Pavia, Pavia; Italy.
[69(a)]INFN Sezione di Pisa;[(b)]Dipartimento di Fisica E. Fermi, Università di Pisa, Pisa; Italy.
[70(a)]INFN Sezione di Roma;[(b)]Dipartimento di Fisica, Sapienza Università di Roma, Roma; Italy.
[71(a)]INFN Sezione di Roma Tor Vergata;[(b)]Dipartimento di Fisica, Università di Roma Tor Vergata, Roma; Italy.
[72(a)]INFN Sezione di Roma Tre;[(b)]Dipartimento di Matematica e Fisica, Università Roma Tre, Roma; Italy.
[73(a)]INFN-TIFPA;[(b)]Università degli Studi di Trento, Trento; Italy.
[74]Institut für Astro- und Teilchenphysik, Leopold-Franzens-Universität, Innsbruck; Austria.
[75]University of Iowa, Iowa City IA; United States of America.
[76]Department of Physics and Astronomy, Iowa State University, Ames IA; United States of America.
[77]Joint Institute for Nuclear Research, Dubna; Russia.
[78(a)]Departamento de Engenharia Elétrica, Universidade Federal de Juiz de Fora (UFJF), Juiz de Fora;[(b)]Universidade Federal do Rio De Janeiro COPPE/EE/IF, Rio de Janeiro;[(c)]Universidade Federal de São João del Rei (UFSJ), São João del Rei;[(d)]Instituto de Física, Universidade de São Paulo, São Paulo; Brazil.
[79]KEK, High Energy Accelerator Research Organization, Tsukuba; Japan.
[80]Graduate School of Science, Kobe University, Kobe; Japan.
[81(a)]AGH University of Science and Technology, Faculty of Physics and Applied Computer Science, Krakow;[(b)]Marian Smoluchowski Institute of Physics, Jagiellonian University, Krakow; Poland.
[82]Institute of Nuclear Physics Polish Academy of Sciences, Krakow; Poland.
[83]Faculty of Science, Kyoto University, Kyoto; Japan.
[84]Kyoto University of Education, Kyoto; Japan.
[85]Research Center for Advanced Particle Physics and Department of Physics, Kyushu University, Fukuoka ; Japan.
[86]Instituto de Física La Plata, Universidad Nacional de La Plata and CONICET, La Plata; Argentina.
[87]Physics Department, Lancaster University, Lancaster; United Kingdom.
[88]Oliver Lodge Laboratory, University of Liverpool, Liverpool; United Kingdom.
[89]Department of Experimental Particle Physics, Jožef Stefan Institute and Department of Physics, University of Ljubljana, Ljubljana; Slovenia.
[90]School of Physics and Astronomy, Queen Mary University of London, London; United Kingdom.
[91]Department of Physics, Royal Holloway University of London, Egham; United Kingdom.
[92]Department of Physics and Astronomy, University College London, London; United Kingdom.
[93]Louisiana Tech University, Ruston LA; United States of America.
[94]Fysiska institutionen, Lunds universitet, Lund; Sweden.
[95]Centre de Calcul de l'Institut National de Physique Nucléaire et de Physique des Particules (IN2P3), Villeurbanne; France.

[96]Departamento de Física Teorica C-15 and CIAFF, Universidad Autónoma de Madrid, Madrid; Spain.
[97]Institut für Physik, Universität Mainz, Mainz; Germany.
[98]School of Physics and Astronomy, University of Manchester, Manchester; United Kingdom.
[99]CPPM, Aix-Marseille Université, CNRS/IN2P3, Marseille; France.
[100]Department of Physics, University of Massachusetts, Amherst MA; United States of America.
[101]Department of Physics, McGill University, Montreal QC; Canada.
[102]School of Physics, University of Melbourne, Victoria; Australia.
[103]Department of Physics, University of Michigan, Ann Arbor MI; United States of America.
[104]Department of Physics and Astronomy, Michigan State University, East Lansing MI; United States of America.
[105]B.I. Stepanov Institute of Physics, National Academy of Sciences of Belarus, Minsk; Belarus.
[106]Research Institute for Nuclear Problems of Byelorussian State University, Minsk; Belarus.
[107]Group of Particle Physics, University of Montreal, Montreal QC; Canada.
[108]P.N. Lebedev Physical Institute of the Russian Academy of Sciences, Moscow; Russia.
[109]Institute for Theoretical and Experimental Physics (ITEP), Moscow; Russia.
[110]National Research Nuclear University MEPhI, Moscow; Russia.
[111]D.V. Skobeltsyn Institute of Nuclear Physics, M.V. Lomonosov Moscow State University, Moscow; Russia.
[112]Fakultät für Physik, Ludwig-Maximilians-Universität München, München; Germany.
[113]Max-Planck-Institut für Physik (Werner-Heisenberg-Institut), München; Germany.
[114]Nagasaki Institute of Applied Science, Nagasaki; Japan.
[115]Graduate School of Science and Kobayashi-Maskawa Institute, Nagoya University, Nagoya; Japan.
[116]Department of Physics and Astronomy, University of New Mexico, Albuquerque NM; United States of America.
[117]Institute for Mathematics, Astrophysics and Particle Physics, Radboud University Nijmegen/Nikhef, Nijmegen; Netherlands.
[118]Nikhef National Institute for Subatomic Physics and University of Amsterdam, Amsterdam; Netherlands.
[119]Department of Physics, Northern Illinois University, DeKalb IL; United States of America.
[120(a)]Budker Institute of Nuclear Physics, SB RAS, Novosibirsk;[(b)]Novosibirsk State University Novosibirsk; Russia.
[121]Department of Physics, New York University, New York NY; United States of America.
[122]Ohio State University, Columbus OH; United States of America.
[123]Faculty of Science, Okayama University, Okayama; Japan.
[124]Homer L. Dodge Department of Physics and Astronomy, University of Oklahoma, Norman OK; United States of America.
[125]Department of Physics, Oklahoma State University, Stillwater OK; United States of America.
[126]Palacký University, RCPTM, Joint Laboratory of Optics, Olomouc; Czech Republic.
[127]Center for High Energy Physics, University of Oregon, Eugene OR; United States of America.
[128]LAL, Université Paris-Sud, CNRS/IN2P3, Université Paris-Saclay, Orsay; France.
[129]Graduate School of Science, Osaka University, Osaka; Japan.
[130]Department of Physics, University of Oslo, Oslo; Norway.
[131]Department of Physics, Oxford University, Oxford; United Kingdom.
[132]LPNHE, Sorbonne Université, Paris Diderot Sorbonne Paris Cité, CNRS/IN2P3, Paris; France.
[133]Department of Physics, University of Pennsylvania, Philadelphia PA; United States of America.
[134]Konstantinov Nuclear Physics Institute of National Research Centre "Kurchatov Institute", PNPI, St. Petersburg; Russia.

[135]Department of Physics and Astronomy, University of Pittsburgh, Pittsburgh PA; United States of America.
[136(a)]Laboratório de Instrumentação e Física Experimental de Partículas - LIP;[(b)]Departamento de Física, Faculdade de Ciências, Universidade de Lisboa, Lisboa;[(c)]Departamento de Física, Universidade de Coimbra, Coimbra;[(d)]Centro de Física Nuclear da Universidade de Lisboa, Lisboa;[(e)]Departamento de Física, Universidade do Minho, Braga;[(f)]Departamento de Física Teorica y del Cosmos, Universidad de Granada, Granada (Spain);[(g)]Dep Física and CEFITEC of Faculdade de Ciências e Tecnologia, Universidade Nova de Lisboa, Caparica; Portugal.
[137]Institute of Physics, Academy of Sciences of the Czech Republic, Prague; Czech Republic.
[138]Czech Technical University in Prague, Prague; Czech Republic.
[139]Charles University, Faculty of Mathematics and Physics, Prague; Czech Republic.
[140]State Research Center Institute for High Energy Physics, NRC KI, Protvino; Russia.
[141]Particle Physics Department, Rutherford Appleton Laboratory, Didcot; United Kingdom.
[142]IRFU, CEA, Université Paris-Saclay, Gif-sur-Yvette; France.
[143]Santa Cruz Institute for Particle Physics, University of California Santa Cruz, Santa Cruz CA; United States of America.
[144(a)]Departamento de Física, Pontificia Universidad Católica de Chile, Santiago;[(b)]Departamento de Física, Universidad Técnica Federico Santa María, Valparaíso; Chile.
[145]Department of Physics, University of Washington, Seattle WA; United States of America.
[146]Department of Physics and Astronomy, University of Sheffield, Sheffield; United Kingdom.
[147]Department of Physics, Shinshu University, Nagano; Japan.
[148]Department Physik, Universität Siegen, Siegen; Germany.
[149]Department of Physics, Simon Fraser University, Burnaby BC; Canada.
[150]SLAC National Accelerator Laboratory, Stanford CA; United States of America.
[151]Physics Department, Royal Institute of Technology, Stockholm; Sweden.
[152]Departments of Physics and Astronomy, Stony Brook University, Stony Brook NY; United States of America.
[153]Department of Physics and Astronomy, University of Sussex, Brighton; United Kingdom.
[154]School of Physics, University of Sydney, Sydney; Australia.
[155]Institute of Physics, Academia Sinica, Taipei; Taiwan.
[156(a)]E. Andronikashvili Institute of Physics, Iv. Javakhishvili Tbilisi State University, Tbilisi;[(b)]High Energy Physics Institute, Tbilisi State University, Tbilisi; Georgia.
[157]Department of Physics, Technion, Israel Institute of Technology, Haifa; Israel.
[158]Raymond and Beverly Sackler School of Physics and Astronomy, Tel Aviv University, Tel Aviv; Israel.
[159]Department of Physics, Aristotle University of Thessaloniki, Thessaloniki; Greece.
[160]International Center for Elementary Particle Physics and Department of Physics, University of Tokyo, Tokyo; Japan.
[161]Graduate School of Science and Technology, Tokyo Metropolitan University, Tokyo; Japan.
[162]Department of Physics, Tokyo Institute of Technology, Tokyo; Japan.
[163]Tomsk State University, Tomsk; Russia.
[164]Department of Physics, University of Toronto, Toronto ON; Canada.
[165(a)]TRIUMF, Vancouver BC;[(b)]Department of Physics and Astronomy, York University, Toronto ON; Canada.
[166]Division of Physics and Tomonaga Center for the History of the Universe, Faculty of Pure and Applied Sciences, University of Tsukuba, Tsukuba; Japan.
[167]Department of Physics and Astronomy, Tufts University, Medford MA; United States of America.
[168]Department of Physics and Astronomy, University of California Irvine, Irvine CA; United States of

America.
[169]Department of Physics and Astronomy, University of Uppsala, Uppsala; Sweden.
[170]Department of Physics, University of Illinois, Urbana IL; United States of America.
[171]Instituto de Física Corpuscular (IFIC), Centro Mixto Universidad de Valencia - CSIC, Valencia; Spain.
[172]Department of Physics, University of British Columbia, Vancouver BC; Canada.
[173]Department of Physics and Astronomy, University of Victoria, Victoria BC; Canada.
[174]Fakultät für Physik und Astronomie, Julius-Maximilians-Universität Würzburg, Würzburg; Germany.
[175]Department of Physics, University of Warwick, Coventry; United Kingdom.
[176]Waseda University, Tokyo; Japan.
[177]Department of Particle Physics, Weizmann Institute of Science, Rehovot; Israel.
[178]Department of Physics, University of Wisconsin, Madison WI; United States of America.
[179]Fakultät für Mathematik und Naturwissenschaften, Fachgruppe Physik, Bergische Universität Wuppertal, Wuppertal; Germany.
[180]Department of Physics, Yale University, New Haven CT; United States of America.
[181]Yerevan Physics Institute, Yerevan; Armenia.
[a] Also at Borough of Manhattan Community College, City University of New York, NY; United States of America.
[b] Also at Centre for High Performance Computing, CSIR Campus, Rosebank, Cape Town; South Africa.
[c] Also at CERN, Geneva; Switzerland.
[d] Also at CPPM, Aix-Marseille Université, CNRS/IN2P3, Marseille; France.
[e] Also at Département de Physique Nucléaire et Corpusculaire, Université de Genève, Genève; Switzerland.
[f] Also at Departament de Fisica de la Universitat Autonoma de Barcelona, Barcelona; Spain.
[g] Associated at Departamento de Física Teorica y del Cosmos, Universidad de Granada, Granada (Spain); Spain.
[h] Also at Departamento de Física Teorica y del Cosmos, Universidad de Granada, Granada (Spain); Spain.
[i] Also at Department of Applied Physics and Astronomy, University of Sharjah, Sharjah; United Arab Emirates.
[j] Also at Department of Financial and Management Engineering, University of the Aegean, Chios; Greece.
[k] Also at Department of Physics and Astronomy, University of Louisville, Louisville, KY; United States of America.
[l] Also at Department of Physics and Astronomy, University of Sheffield, Sheffield; United Kingdom.
[m] Also at Department of Physics, California State University, Fresno CA; United States of America.
[n] Also at Department of Physics, California State University, Sacramento CA; United States of America.
[o] Also at Department of Physics, King's College London, London; United Kingdom.
[p] Also at Department of Physics, St. Petersburg State Polytechnical University, St. Petersburg; Russia.
[q] Also at Department of Physics, Stanford University; United States of America.
[r] Also at Department of Physics, University of Fribourg, Fribourg; Switzerland.
[s] Also at Department of Physics, University of Michigan, Ann Arbor MI; United States of America.
[t] Also at Dipartimento di Fisica E. Fermi, Università di Pisa, Pisa; Italy.
[u] Also at Giresun University, Faculty of Engineering, Giresun; Turkey.
[v] Also at Graduate School of Science, Osaka University, Osaka; Japan.
[w] Also at Hellenic Open University, Patras; Greece.
[x] Also at Horia Hulubei National Institute of Physics and Nuclear Engineering, Bucharest; Romania.
[y] Also at II. Physikalisches Institut, Georg-August-Universität Göttingen, Göttingen; Germany.

[z] Also at Institucio Catalana de Recerca i Estudis Avancats, ICREA, Barcelona; Spain.
[aa] Also at Institut für Experimentalphysik, Universität Hamburg, Hamburg; Germany.
[ab] Also at Institute for Mathematics, Astrophysics and Particle Physics, Radboud University Nijmegen/Nikhef, Nijmegen; Netherlands.
[ac] Also at Institute for Particle and Nuclear Physics, Wigner Research Centre for Physics, Budapest; Hungary.
[ad] Also at Institute of Particle Physics (IPP); Canada.
[ae] Also at Institute of Physics, Academia Sinica, Taipei; Taiwan.
[af] Also at Institute of Physics, Azerbaijan Academy of Sciences, Baku; Azerbaijan.
[ag] Also at Institute of Theoretical Physics, Ilia State University, Tbilisi; Georgia.
[ah] Also at Istanbul University, Dept. of Physics, Istanbul; Turkey.
[ai] Also at LAL, Université Paris-Sud, CNRS/IN2P3, Université Paris-Saclay, Orsay; France.
[aj] Also at Louisiana Tech University, Ruston LA; United States of America.
[ak] Also at Manhattan College, New York NY; United States of America.
[al] Also at Moscow Institute of Physics and Technology State University, Dolgoprudny; Russia.
[am] Also at National Research Nuclear University MEPhI, Moscow; Russia.
[an] Also at Physikalisches Institut, Albert-Ludwigs-Universität Freiburg, Freiburg; Germany.
[ao] Also at School of Physics, Sun Yat-sen University, Guangzhou; China.
[ap] Also at The City College of New York, New York NY; United States of America.
[aq] Also at The Collaborative Innovation Center of Quantum Matter (CICQM), Beijing; China.
[ar] Also at Tomsk State University, Tomsk, and Moscow Institute of Physics and Technology State University, Dolgoprudny; Russia.
[as] Also at TRIUMF, Vancouver BC; Canada.
[at] Also at Universita di Napoli Parthenope, Napoli; Italy.
[*] Deceased